JIPB Journal of Integrative Plant Biology

Research Article
https://doi.org/10.1111/jipb.13504

DIW1 encoding a clade I PP2C phosphatase negatively regulates drought tolerance by de-phosphorylating TaSnRK1.1 in wheat[oo]

Jingyi Wang[1†*], Chaonan Li[1†], Long Li[1†], Lifeng Gao[1], Ge Hu[1], Yanfei Zhang[1], Matthew P. Reynolds[2], Xueyong Zhang[1], Jizeng Jia[1], Xinguo Mao[1*] and Ruilian Jing[1*]

1. National Key Facility for Crop Gene Resources and Genetic Improvement/Institute of Crop Sciences, Chinese Academy of Agricultural Sciences, Beijing 100081, China
2. International Maize and Wheat Improvement Center, Texcoco 56237, Mexico
†These authors contributed equally to this work.
*Correspondences: Ruilian Jing (jingruilian@caas.cn); Xinguo Mao (maoxinguo@caas.cn); Jingyi Wang (wangjingyi@caas.cn; Dr. Wang is fully responsible for the distributions of all materials associated with this article)

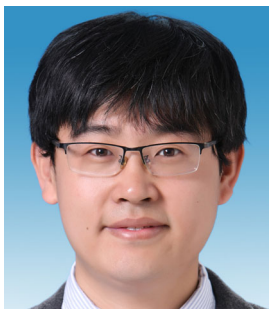

Jingyi Wang

ABSTRACT

Drought seriously impacts wheat production (*Triticum aestivum* L.), while the exploitation and utilization of genes for drought tolerance are insufficient. Leaf wilting is a direct reflection of drought tolerance in plants. Clade A PP2Cs are abscisic acid (ABA) co-receptors playing vital roles in the ABA signaling pathway, regulating drought response. However, the roles of other clade PP2Cs in drought tolerance, especially in wheat, remain largely unknown. Here, we identified a gain-of-function *drought-induced wilting 1* (*DIW1*) gene from the wheat Aikang 58 mutant library by map-based cloning, which encodes a clade I protein phosphatase 2C (TaPP2C158) with enhanced protein phosphatase activity. Phenotypic analysis of overexpression and CRISPR/Cas9 mutant lines demonstrated that DIW1/TaPP2C158 is a negative regulator responsible for drought resistance. We found that TaPP2C158 directly interacts with TaSnRK1.1 and de-phosphorylates it, thus inactivating the TaSnRK1.1–TaAREB3 pathway. TaPP2C158 protein phosphatase activity is negatively correlated with ABA signaling. Association analysis suggested that C-terminal variation of TaPP2C158 changing protein phosphatase activity is highly correlated with the canopy temperature, and seedling survival rate under drought stress. Our data suggest that the favorable allele with lower phosphatase activity of TaPP2C158 has been positively selected in Chinese breeding history. This work benefits us in understanding the molecular mechanism of wheat drought tolerance, and provides elite genetic resources and molecular markers for improving wheat drought tolerance.

Keywords: association analysis, drought, elite genetic resources, map-based clone, PP2C, protein phosphatase, wheat, wilting

Wang, J., Li, C., Li, L., Gao, L., Hu, G., Zhang, Y., Reynolds, M. P., Zhang, X., Jia, J., Mao, X., et al. (2023). *DIW1* encoding a clade I PP2C phosphatase negatively regulates drought tolerance by de-phosphorylating TaSnRK1.1 in wheat. J. Integr. Plant Biol. **65:** 1918–1936.

INTRODUCTION

Wheat (*Triticum aestivum* L.) is one of the staple food crops in the world, providing ~20% of protein and calories for humans (Shiferaw et al., 2013). However, it is mainly grown in arid and semi-arid areas (Lesk et al., 2016), and often suffers from drought stress (DS). Therefore, an understanding of the adaptation mechanism of wheat to

water stress and breeding drought-tolerant cultivars with high and stable yields is needed to cope with climate change and ensure food security for the growing population (Tester and Langridge, 2010; Park et al., 2015).

However, drought tolerance is a quantitative trait controlled by multiple genes through complex molecular mechanisms (Tardieu et al., 2018). Abscisic acid (ABA), an essential plant hormone, plays a central role in this process (Fujii et al., 2009; Cutler et al., 2010). The canonical core ABA signaling module consisting of PYR1/PYLs (PYRABACTIN RESISTANCE/PYR1-Like)/RCARs (Regulatory Components of ABA Receptors)–PP2Cs (clade A protein phosphatases type 2C)–SnRK2s (sucrose nonfermenting 1-related protein kinase 2) has been intensively studied in many plant species, especially in the model plant Arabidopsis (Ma et al., 2009; Melcher et al., 2009; Park et al., 2009; Santiago et al., 2009; Brandt et al., 2012). The clade A PP2Cs, such as ABI1 (ABA Insensitive 1) and ABI2 are ABA co-receptors that are negative regulators directly interacting with and inhibiting SnRK2s under normal growth conditions. When ABA accumulates under DS, PYLs bind ABA, and interact with the clade A PP2Cs to release the inhibitory effect of PP2Cs on SnRK2s (Ma et al., 2009; Park et al., 2009). Several recent studies indicated that DS could activate RAF-like kinases, which can phosphorylate and activate SnRK2s (Fabregas et al., 2020; Katsuta et al., 2020; Lin et al., 2020; Takahashi et al., 2020), thus triggering ABA signaling transduction (Gong et al., 2020; Chen et al., 2021). Wheat PP2Cs can be categorized into 13 clades (A–M) (Yu et al., 2019). However, ABA signaling pathway in wheat and the functions of other clade PP2Cs remain unclear (Yu et al., 2020; Guo et al., 2022). As for SnRKs, most studies have focused on the functions of the SnRK2 subfamily members in stress tolerance (Soon et al., 2012), at this time accumulating evidence has shown that SnRK1s act as convergence points of various energy, metabolism, hormone, and stress signals (especially ABA) during growth and development (Baena-Gonzalez et al., 2007; Polge and Thomas, 2007; Jossier et al., 2009; Lin et al., 2014).

Leaf wilting reflects the stomata and transpiration status of plants under drought conditions, and is an essential characteristic of drought response. For example, in *Arabidopsis*, *LEW1* and *LEW3* (*leaf wilting 1* and *3*) genes play crucial roles in the abiotic stress response, and their mutants have a leaf-wilting phenotype (Zhang et al., 2008a, 2009). In soybean, slow canopy wilting is considered a promising indicator for improving drought tolerance compared with fast canopy wilting (FW) plants (Ye et al., 2020). Most mutants of positive regulators, such as SLAC1, OST1, and GHR1, in ABA-mediated stomatal movement or *abi1-1* and *abi2-1* mutants, whose mutations have lost their interaction and inhibition by PYLs, exhibit earlier leaf-wilting phenotypes under DS (Mustilli et al., 2002; Negi et al., 2008; Vahisalu et al., 2008; Hua et al., 2012; Chen et al., 2021; Zhang et al., 2022). Therefore, screening leaf-wilting mutants under drought is an effective way to clone drought-related genes using CRISPR/Cas9 gene editing techniques to improve crop drought resistance (Zhu et al., 2020).

To date, only a few genes related to drought tolerance have been reported in wheat, such as *TaPYLs* and *TaSNAC8-6A* through gene family analysis (Mega et al., 2019; Mao et al., 2020, 2022a), *TaHXK3* and *TaNAC071-A* in a genome-wide association study (Li et al., 2022; Mao et al., 2022b), and *DREB/CBF* by yeast-one-hybrid screening (Yang et al., 2020). Although there have been many reports on mapping of quantitative trait loci (QTL) or genes responsible for drought tolerance in wheat, no QTL or related genes have been cloned by map-based cloning (Fleury et al., 2010; Gahlaut et al., 2017).

The present study identified a wheat *drought-induced wilting 1* (*diw1-1*) mutant. Map-based cloning identified the *DIW1* gene that encodes a clade I PP2C phosphatase, named *TaPP2C158*. We found that *diw1-1 is* a gain-of-function mutant with increasing phosphatase activity. TaPP2C158 interacts with TaSnRK1.1 to co-regulate the drought response of wheat. We found the favorable allele of *TaPP2C158* in wheat accessions and developed its molecular markers for the genetic improvement of drought tolerance.

RESULTS

A mutant *diw1-1* exhibits ABA-insensitive and drought-sensitive phenotypes

To isolate uncharacterized drought-related mutants, we screened an M_2 population of wheat variety Aikang 58 (AK58) mutated using ethyl methanesulfonate under DS. Wheat seedlings were cultured under normal conditions for ~4 weeks. Then the three-leaf seedlings were subjected to water withholding for 2 weeks. One *diw1-1* mutant was isolated that showed no apparent phenotypic difference under normal growth conditions (Figure 1A). We backcrossed *diw1-1* twice to the wild-type AK58, and then performed the following experiments. The leaf rolling index (LRI) of the second fully extended leaf was used to quantify the leaf-wilting degree. The LRIs of *diw1-1* were significantly higher than that of AK58 after 14 d of drought treatment (Figure 1B). The water loss rate of detached shoots of *diw1-1* was also much faster than that of AK58 (Figure 1C). In addition, under drought treatment, the stomatal aperture of the *diw1-1* abaxial epidermis was larger than that of AK58 (Figure 1D, E). Given that ABA plays a vital role in plant drought tolerance, we then detected the ABA sensitivity of *diw1-1*. When seeds were treated with 20 μM ABA during germination, *diw1-1* exhibited more tolerance to ABA than the wild-type (Figure 1F, G). After seeds were germinated in water for 2 d, seedlings were transferred into a pouch containing 30 μM ABA. We observed that the primary root growth of the *diw1-1* mutant was much less inhibited by 30 μM ABA than that of the wild-type (Figure 1H, I). These results demonstrated that *diw1-1* shows a drought-sensitive, but ABA-insensitive, phenotype.

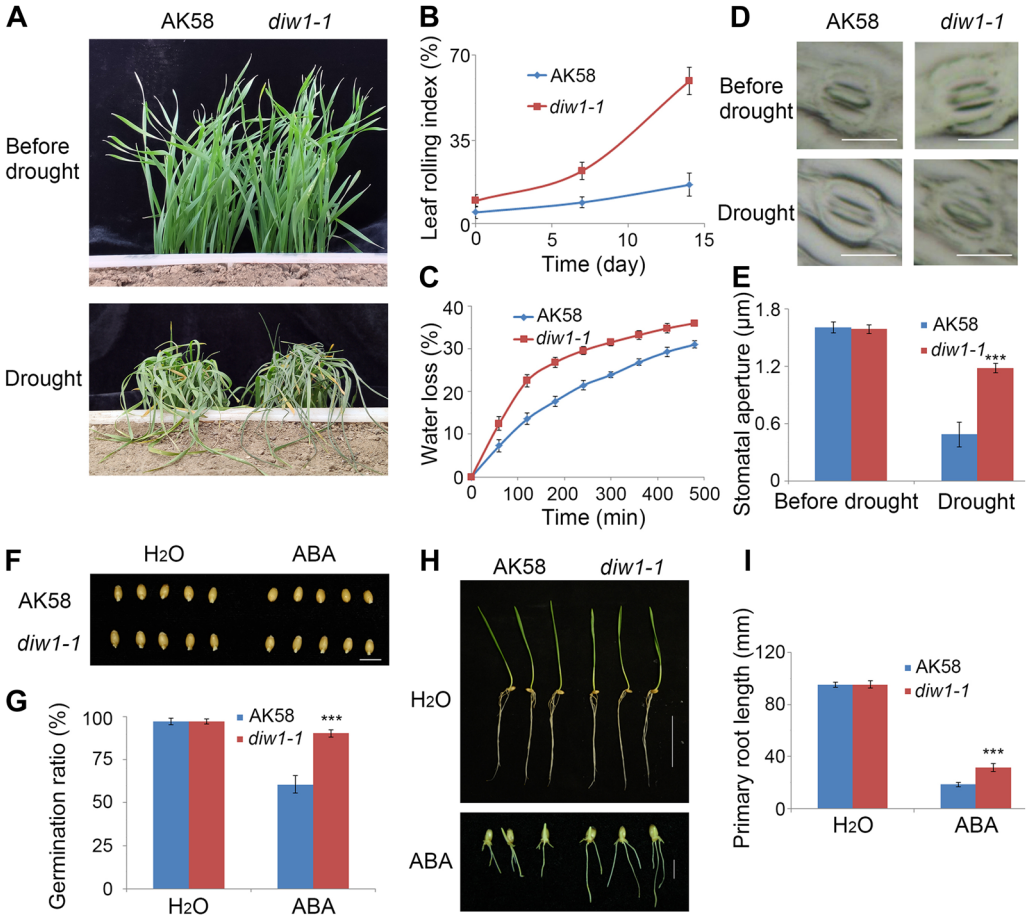

Figure 1. *diw1-1* mutant is sensitive to drought stress (DS) and insensitive to abscisic acid (ABA)
(A) The seedling phenotypes of *diw1-1* mutant and wild-type AK58 before and after drought treatment. Seedlings with three leaves were subjected to DS by withholding water for 14 d. **(B)** Leaf rolling index of *diw1-1* and AK58 under drought treatment. The second fully extended leaves of at least 10 seedlings were detected per replicate. **(C)** Comparison of detached leaf water loss of *diw1-1* and AK58. Shoots of three seedlings with three leaves were detached to measure water loss under room temperature conditions. **(D)** Representative stomata of the second fully extended leaf abaxial epidermis before or 14 d after drought treatment. Bars = 10 μm. **(E)** Statistical analyses of the stomatal aperture are shown in **(D)**. At least 30 stomatal apertures were measured per replicate. **(F)** Effects of 20 μM ABA on germination of *diw1-1* and AK58 seeds. Bar = 1 cm. **(G)** Statistical analyses of *diw1-1* and AK58 seeds germination ratio shown in **(F)**. At least 30 seeds were counted in each experiment. **(H)** Primary root growth of *diw1-1* is insensitive to ABA. After germination in water for 2 d, seeds were transferred to a seed germination pouch and grown for 7 d with or without 30 μM ABA. Upper bar = 5 cm, lower bar = 1 cm. **(I)** Statistical analyses of primary root length in **(H)**. Nine seedlings were collected from three germination pouches. All the above experiments were performed three times independently. Data represent means ± SE. ***, *t*-test with $P < 0.001$.

TaPP2C158 is the candidate gene of *diw1-1*

To clone the *DIW1* gene, we crossed the *diw1-1* mutant onto the AK58 background with a wheat variety Zhongmai 36 (ZM36) to obtain the F_2 population. Four-week-old seedlings were treated by water withholding for 2 weeks. The proportion of individuals exhibiting a low, moderate, or severe wilting phenotype in the F_2 population was 1:2:1 (Figure S1), suggesting that *diw1-1* is a semi-dominant mutant. Two pools of extreme phenotypic seedlings exhibiting low and severe wilting and two parents, AK58 and ZM36, were genotyped using a Wheat 660 K SNP array. A total of 80,363 high-resolution polymorphic sites was identified between the two parents whereas, in the severe wilting pool, 1693 sites were the same genotype as AK58 (*diw1-1*). A series of polymorphic loci associated with wilting phenotypes was detected throughout the genome (Figure S2). A highly dense region of SNP markers closely associated with the wilting phenotype was identified between 560 and 564 Mbp on chromosome 5A (Figure 2A). This result suggests that the mutant gene is located in the chromosome region where the AK58 genome sequence shows good co-linearity with that of Chinese Spring (CS) (Figure 2B, C). The *diw1-1* seedlings with the severe wilting phenotype were screened from the F_2 population of ~15,000 plants. Among them, ~10% of the seedlings showed recombination at both marker sites, Sites 5A-97 and 5A-16, and were considered false *diw1-1* plants. Finally, 2859 *diw1-1* seedlings with the wilting phenotype were used for map-based cloning of the target gene. *DIW1* was located within a 43.4-kbp region between markers 5A-2 and 5A-4 on chromosome 5A. In total, three genes were predicted in this region (Table S1). We sequenced the three candidate genes and

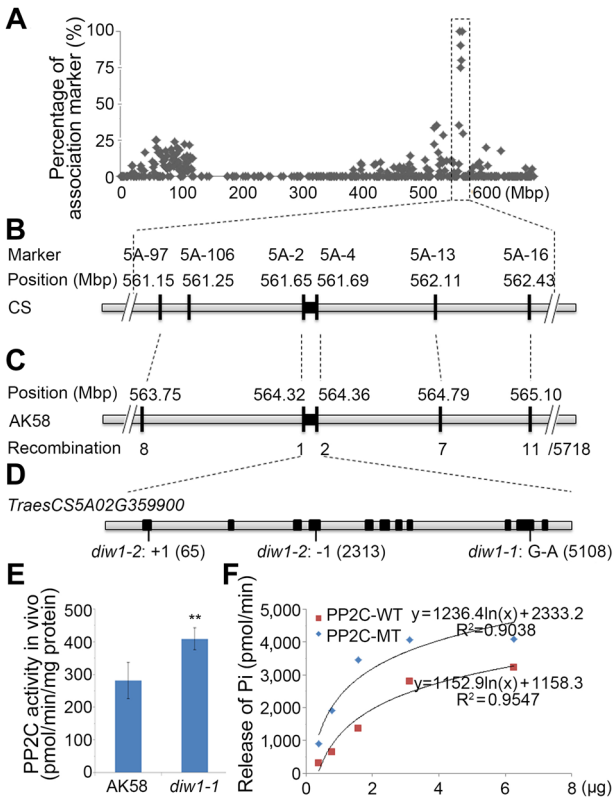

Figure 2. Map-based cloning of *DIW1* and comparison of PP2C phosphatase activity

(A) Percentage of SNP markers associated with wilting phenotype on chromosome 5A. The dotted rectangular box indicates the candidate gene region. **(B, C)** The candidate gene region of Chinese Spring (CS) is syntenic with the region of AK58, and has the same markers, which are indicated by dashed lines. The black rectangle represents the target region harboring *DIW1*. Vertical lines indicate mapping marker locations. The numbers below the vertical lines indicate the number of recombinants. **(D)** Gene structure of *DIW1*. Black rectangles indicate exons. A G-to-A mutation at position 5108 (*diw1-1*) and two InDels at positions 65 and 2313 (*diw1-2*) in *TraesCS5A02G359900* are indicated. **(E)** Total PP2C activity in *diw1-1* and wild-type. Total proteins were extracted from 4-week-old seedlings. PP2C activity is represented as the amount of phosphate dephosphorylated by PP2C released per minute, after adding 5 mM okadaic acid to inhibit the activity of PPP family Ser/Thr-specific phosphoprotein phosphatases. The release of Pi was measured using the Ser/Thr Phosphatase Assay Kit. Three independent experiments were performed with similar results. Data represent means ± SE. **, *t*-test with $P < 0.01$. **(F)** Different TaPP2C form phosphatase activity assay *in vitro* using recombinant proteins of PP2C-WT and PP2C-MT. The experiments were performed three times with similar results.

identified only a G5108A substitution in *TraesCS5A02G359900* (counting from the first putative ATG initiation codon) (Figure 2D), which resulted in conversion of glutamate (E364, GAA) to lysine (K364, AAA). *TraesCS5A02G359900* encodes a clade I protein phosphatase 2C, previously named TaPP2C158 (Yu et al., 2019) (Figure S3).

The mutation enhances the protein phosphatase activity of PP2Cs

Because the candidate gene of *diw1-1* is a PP2C phosphatase, we first detected the total activity of PP2C in AK58 and *diw1-1* seedlings using okadaic acid, which is ineffective toward PP2C but could inhibit the activity of other protein phosphatase family members (Wang et al., 2018b). As shown in Figure 2E, the *diw1-1* mutant showed a higher PP2C activity than AK58, which is consistent with the ABA-insensitive phenotype. To further determine whether an amino acid change between PP2C-WT (TaPP2C158 cloned from wild-type AK58) and PP2C-MT (TaPP2C158 cloned from *diw1-1* mutant) proteins caused wilting phenotype under DS, the protein phosphatase activity of PP2C-WT and PP2C-MT was measured *in vitro*. We expressed His-tagged PP2C-WT and PP2C-MT in *Escherichia coli*, and checked their PP2C activity. As shown in Figure 2F, PP2C-MT had higher protein phosphatase activity than PP2C-WT. Based on the fact that this single amino acid mutation enhanced PP2C activity *in vivo* and *in vitro*, we speculate that *diw1-1* is a gain-of-function mutation.

DIW1/TaPP2C158 is responsible for drought response

To further confirm that the *diw1-1* is a gain-of-function mutation that harbors an amino acid mutation in *TaPP2C158*, we constructed and introduced an overexpression *TaPP2C-MT* cDNA vector into a wheat cultivar Fielder via *Agrobacterium tumefaciens*-mediated transformation. The *TaPP2C158* expression levels in independent homozygous T_3 lines were detected (Figure S4). Simultaneously, we constructed CRISPR/Cas9 lines in which two target sites were designed (Figure S5) (Wang et al., 2015). Mutants edited only in genome A but not in genomes B and D were selected for further study. The *diw1-2* mutant has a 1-bp insertion at the 65-bp position (counting from the first putative ATG initiation codon) and a 1-bp deletion at 2,313 bp, both of which would create a stop codon. The *diw1-3* mutant has a 2.2-kb deletion between the target Sites 1 and 2, and the *diw1-4* mutant has a 3-bp deletion in target Site 1 and a 1-bp insertion in target Site 2. As *diw1-2*, *diw1-3*, and *diw1-4* mutants had similar phenotypes, such as wilting, LRI, water loss rate, stomatal aperture, and ABA sensitivity, *diw1-2* was selected as the representative for further study. Under drought treatment for 18 d, the wild-type Fielder plants showed a less wilting phenotype than *PP2C-MT-OE2* and *PP2C-MT-OE5*, but a more wilting phenotype than *diw1-2* (Figure 3A, B).

Furthermore, the water loss rate was the fastest in *PP2C-MT-OE* lines, faster in Fielder than in *diw1-2* (Figure 3C). Accordingly, under drought treatment for 18 d, the stomatal aperture of the abaxial epidermis was the largest in the *PP2C-MT-OE* lines, and larger in Fielder than that of *diw1-2* (Figure 3D). *PP2C-MT-OE*s showed an ABA-insensitive phenotype, while *diw1-2* showed an ABA-sensitive phenotype in seed germination and primary root growth (Figure 3E–H). These results suggested that *TaPP2C158* is a negative regulator for drought tolerance.

Next, we investigated the spatial expression pattern of *TaPP2C158* and found that *TaPP2C158* was constitutively expressed in wheat tissues (roots and leaves of seedlings; roots, stems, flag leaves, and spikes at the flowering stage), but expressed preferentially in roots at the seedling stage

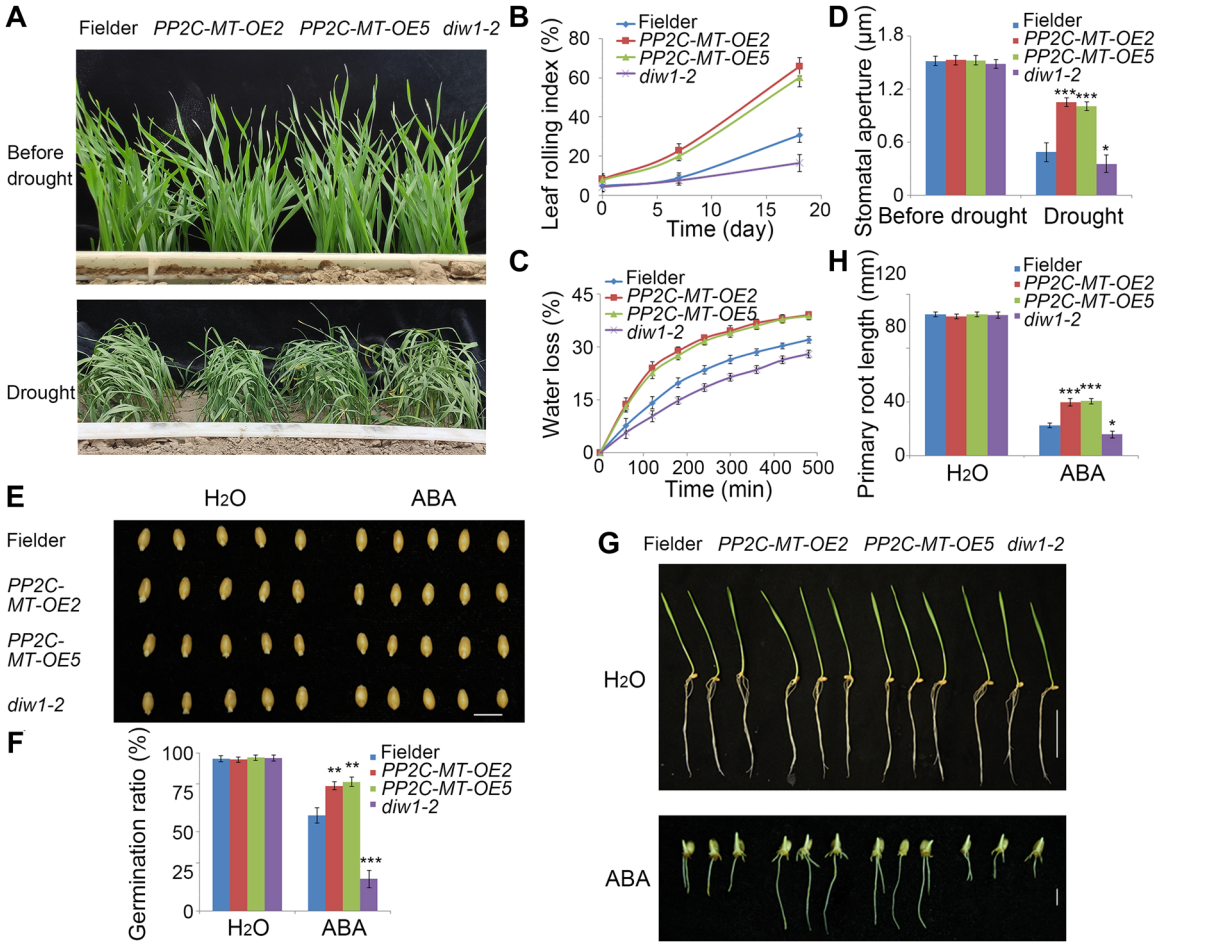

Figure 3. Phenotypes of *TaPP2C-MT* overexpression lines and mutants

(A) The seedling phenotype of Fielder, *PP2C-MT-OE2*, *PP2C-MT-OE5*, and *diw1-2* before and after drought treatment. Four-week-old seedlings were subjected to DS by withholding water for 18 d. **(B)** Leaf rolling index during drought treatment. The second fully extended leaves of at least 10 seedlings were detected per replicate. **(C)** Relative water loss. Shoots of 4-week-old plants of three seedlings were detached and used for water loss measurements. **(D)** The stomatal aperture of the second fully extended leaf abaxial epidermis before or under drought treatment for 18 d. At least 30 stomata were measured per replicate. **(E)** Photographs showing seed germination of *TaPP2C-MT* overexpression lines and mutants seeds with or without 20 μM abscisic acid (ABA). Bar = 1 cm. **(F)** Statistical analysis of seed germination ratio shown in **(E)**. For each replicates, at least 30 seeds were counted. **(G)** Primary root growth with or without ABA. After 2 d of germination in water, seeds were transferred to seed germination pouches and grown for 7 d with or without 30 μM ABA. Upper bar = 5 cm, lower bar = 1 cm. **(H)** Statistical analysis of primary root length in **(G)**. Nine seedlings were collected from three germination pouches. All the above experiments were performed three times independently. Data represent the means ± SE. *, *t*-test with $P < 0.05$. **, *t*-test with $P < 0.01$. ***, *t*-test with $P < 0.001$.

(Figure S6A). We further examined the expression pattern of *TaPP2C158* under ABA treatment. Real-time PCR results showed that *TaPP2C158* was induced by ABA treatment at different time points (Figure S6B). Previous studies have shown that all eight clade A PP2Cs in wheat were induced by ABA (Yu et al., 2019). These results indicated that TaPP2C158 may be similar to the clade A PP2Cs, regulating the homeostasis of ABA signaling via a feedback loop, but with an unknown mechanism (Wang et al., 2019c).

As the clade A PP2Cs interact with ABA receptors PYLs and TaPYL4 plays an essential role in the wheat ABA signal (Mega et al., 2019), we checked the interaction of TaPP2C158 with TaPYL4 using a yeast-two-hybrid (Y2H) assay. However, we did not detect any interactions with or without the addition of ABA (Figure S7). We further investigated the subcellular localization of TaPP2C158, by transiently expressing TaPP2C158-GFP in wheat protoplasts and *Nicotiana benthamiana* leaves. Green fluorescence showed TaPP2C158 was localized in the cell membrane, cytoplasm, and nucleus (Figure S8).

TaPP2C158 interacts with TaSnRK1.1

To understand how TaPP2C158 participates in abiotic stress tolerance, we used *TaPP2C158* as baits in Y2H to screen a prey library of stress-treated wheat seedlings (Wang et al., 2019a). More than 3.0×10^7 independent clones were screened, and 1,248 clones were selected for sequencing. In total, 480 fragments were obtained with 297 predicted sequences in the frame, and annotated as 45 proteins (Table S2). Among them, *TaSnRK1.1* was identified as a candidate interactor six times. Furthermore, we cloned *TaSnRK1.1* full-length

cDNA from AK58 and confirmed the interaction between TaPP2C158 and TaSnRK1.1 using the Y2H assay (Figure 4A). Next, a luciferase complementation imaging (LCI) assay was performed in *N. benthamiana* leaves via *Agrobacterium* infiltration. A strong luminescence signal was only observed in the area co-expressing TaSnRK1.1-nLUC and TaPP2C158-cLUC (Figure 4B). We also infiltrated tobacco leaves transiently co-expressing TaPP2C158-GFP with TaSnRK1.1-Flag for co-immunoprecipitation (Co-IP) assays. Using anti-GFP magnetic beads to immunoprecipitate protein, immune-blot assays with anti-Flag antibodies showed that TaPP2C158 interacted with TaSnRK1.1 (Figure 4C). Finally, a bimolecular fluorescence complementation (BiFC) assay was performed in *N. benthamiana* leaves following *Agro*-infiltration of a YCE/YNE fusion of TaPP2C158 and TaSnRK1.1. A strong YFP signal was only detected in the combination of co-expressing TaPP2C158-YCE and TaSnRK1.1-YNE (Figure 4D). Overall, Y2H, LCI, Co-IP, and BiFC assays confirmed the interaction between TaPP2C158 and TaSnRK1.1.

TaPP2C158 blocks the drought response by de-phosphorylating and inactivating TaSnRK1.1

To evaluate the effect of the TaPP2C158-TaSnRK1.1 interaction on the de-phosphorylation of TaSnRK1.1, we expressed recombinant His-tagged TaPP2C158 and GST-tagged TaSnRK1.1 *in vitro*. TaSnRK1.1 exhibited auto-phosphorylation activity in the presence of ATP by delayed mobility in a Phos-tag SDS-PAGE. PP2C-WT treatment caused a partial de-phosphorylation of TaSnRK1.1, while PP2C-MT treatment caused almost complete de-phosphorylation of TaSnRK1.1 (Figure 5A). These results indicated that PP2C-WT and PP2C-MT can de-phosphorylate TaSnRK1.1, while PP2C-MT has a stronger protein phosphatase activity than PP2C-WT, which further confirmed our previous results.

To clarify the effect of endogenous *TaPP2C158* deficiency on downstream TaSnRK1.1 *in vivo*, we detected the phosphorylation level of TaSnRK1.1 in the *diw1-2* mutant. An empty pCAMBIA1300 vector containing Flag-tag and a pCAMBIA1300 vector fused with *TaSnRK1.1* and Flag-tag were transformed into wild-type Fielder and *diw1-2* wheat protoplasts, separately. The Phos-tag mobility shift assay and immune-blotting analysis showed that phosphorylated and non-phosphorylated TaSnRK1.1-Flag existed in *diw1-2* wheat protoplasts, due to TaPP2C158 deficiency. Only non-phosphorylated TaSnRK1.1-Flag was detected in wild-type Fielder wheat protoplasts, as TaPP2C158 can de-phosphorylate TaSnRK1.1 *in vivo* (Figure 5B).

Our previous studies have demonstrated that TaSnRK2.10 confers drought tolerance in plants (Zhang et al., 2023). TaPP2C158 can de-phosphorylate TaSnRK1.1, but not TaSnRK2.10 (Figure S9). This suggests that TaPP2C158 is not involved in the core ABA signaling pathway consisting of PYL–PP2C–SnRK2–AREB, but in a branching signaling pathway via TaSnRK1.1 in plants.

Previous studies have proved that ABA enhances SnRK1 activity in wheat roots (Coello et al., 2012). To detect the role of

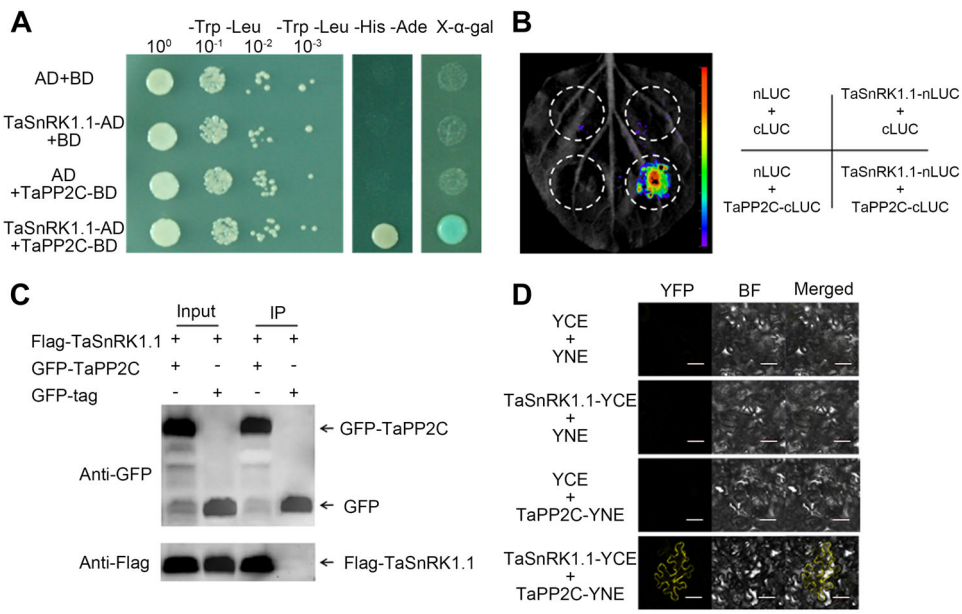

Figure 4. TaPP2C158 interacts with TaSnRK1.1

(A) TaPP2C158 interacts with TaSnRK1.1 in yeast. *TaSnRK1.1* was fused to the pGADT7 vector, and *TaPP2C158* was fused to the pGBKT7 vector. After co-transformation into yeast strain AH109, the transformants were plated onto SD/−Trp−Leu and SD/−Trp−Leu−His−Ade plates with or without X-α-gal. **(B)** Luciferase complementation imaging (LCI) assays showing the interaction of TaPP2C158 with TaSnRK1.1 in *Nicotiana benthamiana*. TaSnRK1.1 was fused to the N-terminal of LUC, and TaPP2C158 was fused to the C-terminal of LUC. **(C)** TaPP2C158 interacts with TaSnRK1.1 in a co-immunoprecipitation (Co-IP) assay in *N. benthamiana*. Total proteins were immunoprecipitated with an anti-GFP affinity gel (GFP-IP), and TaSnRK1.1-Flag was detected with an anti-Flag antibody. **(D)** The interaction of TaPP2C158 and TaSnRK1.1 was verified by bimolecular fluorescence complementation (BiFC) assay. The constructs were co-injected into *N. benthamiana* leaves, and YFP signals were observed after 48 h. Bars = 50 μm.

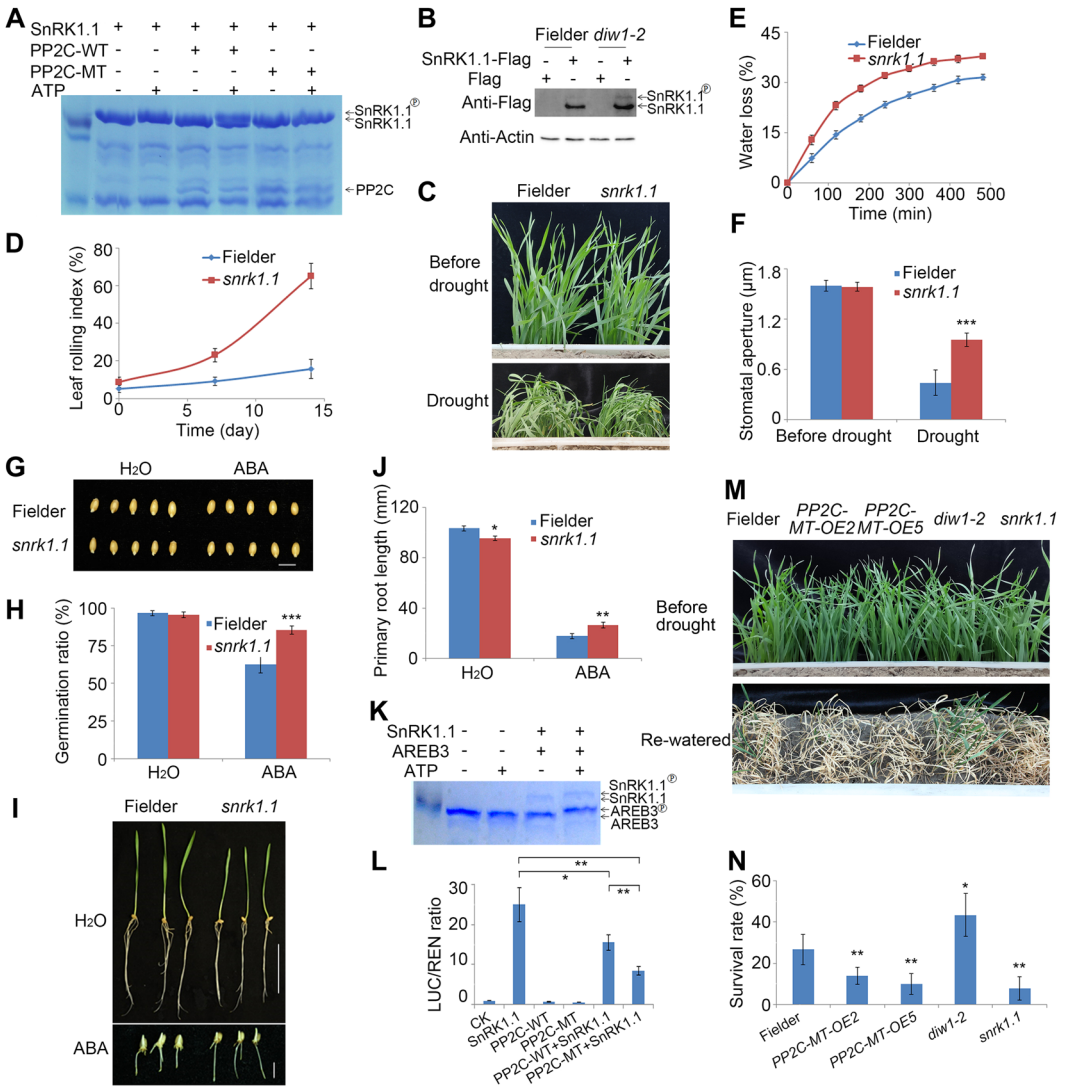

Figure 5. TaPP2C158 blocks the abscisic acid (ABA) signal pathway by phosphorylating and inactivating TaSnRK1.1

(A) TaPP2C158 de-phosphorylates TaSnRK1.1 *in vitro*. Different forms of His tagged PP2C (PP2C-WT and PP2C-MT) were incubated with GST-tagged TaSnRK1.1 with or without ATP, and then analyzed by Phos-tag mobility shift assays. Phosphorylated, non-phosphorylated SnRK1.1, and PP2C proteins are marked. **(B)** Phos-tag mobility shift assay and immune-blotting analysis showed that phosphorylated SnRK1.1-Flag existed in *diw1-2* transformed protoplast, not in wild-type Fielder. **(C)** The seedling phenotype of wild-type Fielder and *snrk1.1* before and after drought treatment. Four-week-old seedlings were subjected to drought stress by withholding water for 14 days. **(D)** Leaf rolling index during drought treatment. The second fully extended leaves of at least ten seedlings were detected per replicate. **(E)** Relative water loss. Shoots of three four-week-old seedlings were detached and used for water loss measurements. **(F)** The stomatal aperture of the second fully extended leaf abaxial epidermis before or under drought treatment for 14 days. At least 30 stomatal apertures were measured per replicate. **(G)** Photograph showing seed germination with or without 20 μM ABA. Bars = 1 cm. **(H)** Statistical analysis of seed germination ratio shown in **(G)**. At least 30 seeds were counted. **(I)** Primary root growth with or without ABA. After two days of germination in water, seeds were transferred to seed germination pouchs and grown for seven days with or without 30 μM ABA. Upper bar = 5 cm, down bar = 1 cm. **(J)** Statistical analysis of primary root length in **(I)**. Nine seedlings were collected from three germination pouchs. **(K)** TaSnRK1.1 phosphorylates TaAREB3 *in vitro*. TaSnRK1.1 and TaAREB3 were incubated with or without ATP, and then analyzed by Phos-tag mobility shift assays. Phosphorylated, and non-phosphorylated SnRK1.1/AREB3 proteins are marked. **(L)** The LUC activity was reduced when *TaSnRK1.1* was co-transformed with *PP2C-WT* or *PP2C-MT*. *pTaRAB18:LUC* was co-transformed with *p35S:SnRK1.1* with or without *PP2C-WT* or *PP2C-MT* to wheat protoplast. Luciferase activity was used to indicate the expression of the ABA-responsive gene *TaRAB18*, and REN was used as an internal control. **(M)** The seedling phenotype of overexpression and mutant lines before and after drought treatment. Seedlings at the 3-leaf stage were withdrawn from watering for 25 days and then re-watered, and photographed on the fifth day after re-watered. **(N)** Seedling survival rates after re-watered. All the above experiments were performed three times independently. Data represent means ± SE. *, t-test with $P < 0.05$. **, *t*-test with $P < 0.01$. ***, *t*-test with $P < 0.001$.

TaSnRK1.1 in the ABA signal pathway, we created a CRISPR/Cas9 line (*snrk1.1*) based on two target sites in *TaSnRK1.1* (Figure S10). Mutants that were edited only in genome A and not in genome B or D were selected for further study. Despite its slow-growing phenotype, the *snrk1.1* mutant showed a similar drought-sensitive phenotype as *diw1-1*, such as a higher LRI, faster water loss rate, and bigger stomatal aperture under drought treatment (Figure 5C–F). The *snrk1.1* mutant also exhibited an ABA-insensitive phenotype during seed germination and primary root growth (Figure 5G–J).

Previous studies have shown that SnRK1.1 could efficiently phosphorylate ABF/AREB (Zhang et al., 2008b; Rodrigues et al., 2013), and that wheat transcription factor TaAREB3 participated in drought tolerance (Wang et al., 2016a). To investigate the effect of TaSnRK1.1 phosphorylation activity, we performed *in vitro* kinase assays. As shown in Figure 5K, TaSnRK1.1 could phosphorylate TaAREB3. These results indicated that TaSnRK1.1 has phosphorylation activity, and TaAREB3 is a substrate.

Previous studies have also shown that the expression of ABA-induced genes can be monitored using the ABA-responsive reporter construct *pRAB18:LUC* (Ma et al., 2009). We identified an *AtRAB18* homologous gene *TaRAB18* (*TraesCS5A02G369800*), and found five ABA response elements (ABREs) in its promoter region, which can be induced by drought (Figure S11). To further investigate the regulation of TaPP2C158 on TaSnRK1.1 in the ABA signal pathway, we used the luciferase assay with *pTaRAB18:LUC* reporter as the readout. In transfected wheat protoplasts, *TaSnRK1.1* overexpression is sufficient to induce strong LUC. The LUC activity was reduced when *TaSnRK1.1* was co-transformed with *PP2C-WT* or *PP2C-MT*. Moreover, the LUC activity of *PP2C-MT* co-transformed with *TaSnRK1.1* was significantly lower than that of *PP2C-WT* (Figure 5L). These results suggested that TaPP2C158 and TaSnRK1.1 jointly regulate the ABA signal pathway in wheat, and that TaPP2C158 protein phosphatase activity is negatively correlated with ABA signaling.

We further examined the survival rate (SR) of overexpression and mutant seedlings under drought conditions. Most seedlings for *PP2C-OE* and *snrk1.1* failed to recover after 25 d of water deprivation, following 5 d of re-watering, while the SRs of Fielder and *diw1-2* plants were 25% and 40%, respectively (Figure 5M, N).

Sequence polymorphism of *TaPP2C158*

TaPP2C158 is involved in wheat drought tolerance. Phenotypes related to drought tolerance, such as seedling SR and canopy temperature (CT), varied significantly among wheat accessions. To identify whether *TaPP2C158* contributed to these phenotypic variations, a 5.4 kb genomic region of *TaPP2C158* from 32 highly diverse wheat accessions was amplified and sequenced separately. Three haplotypes were detected by re-sequencing the *TaPP2C158* gene, named *Hap*1 to *Hap*3, and 21 polymorphic sites were identified, including a 48-bp InDel located at the C-terminus of the *TaPP2C158* coding region, two synonymous SNPs, and 18 SNPs in the intron region (Figure 6A). The three haplotypes can be easily distinguished by molecular markers designed according to the two polymorphic sites, namely SNP at 4221 bp and InDel at 5,048–5,095 bp (Figure 6B, C). These molecular markers were used to detect haplotypes in 323 accessions of the natural wheat population (Population 1) (Table S3). It is worth noting that *Hap*2 and *Hap*3 encode the same protein, whereas the *Hap*1 encodes a different protein with an additional 16 amino acids in the C-terminal end.

A

Hap	836-837	860	1,023	1,148	1,202	1,447	1,574	1,911	1,992	2,363-2,364	2,541	2,720	2,823	3,590-3,591	3,607	3,837	4,221	4,415	4,716	4,881	5,048-5,095
*Hap*1	AC	G	T	T	G	G	T	T	C	--	C	A	C	GG	G	T	T	C	G	G	+
*Hap*2	AC	A	T	C	A	A	C	A	T	CT	G	G	T	G-	A	G	T	T	A	G	-
*Hap*3	TT	G	C	T	G	G	T	T	C	--	G	A	T	T-	G	G	C	C	A	A	-

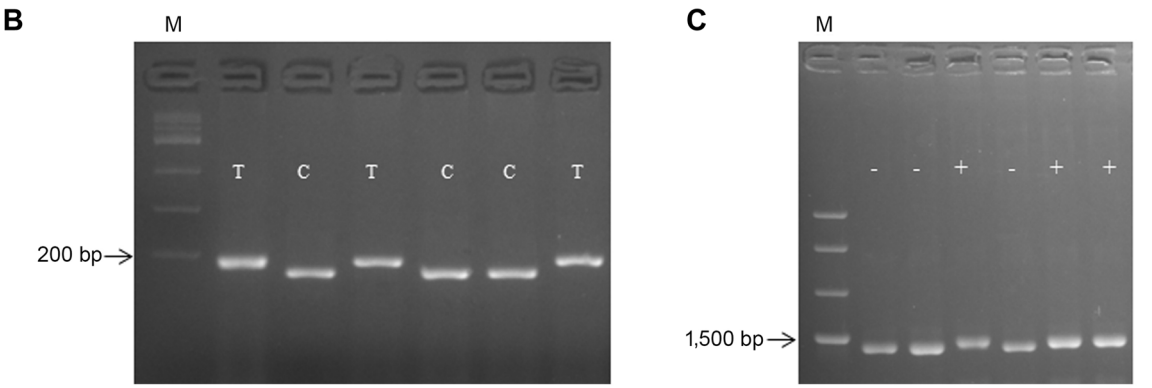

Figure 6. *TaPP2C158* nucleotide polymorphism and its markers

(A) Polymorphic sites detected in the *TaPP2C158* gene region. **(B)** A dCAPS marker developed from a single-nucleotide polymorphism (T/C) at the 4,221-bp site on *TaPP2C158*. The marker contains a mismatched nucleotide in the forward primer that produces a recognition site for the restriction enzyme *Ava*II. The 193-bp fragment amplified from allele **(C)** accessions was digested using *Ava*II, and 163-bp and 30-bp fragments were obtained, whereas the amplified fragment from allele (T) accessions was not digested by *Ava*II. M, 100-bp DNA ladder. **(C)** A PCR marker developed from the InDel at 5,048–5,095 bp. The PCR product length in alleles with the deletion is 1,432 bp, whereas with the insertion it is 1,480 bp. M, Marker III DNA ladder.

Effects of C-terminal variation on wheat CT and seedling SR, and protein phosphatase activity *in vitro*

Association analysis of two polymorphic loci and CT, seedling SRs in the full panel of 323 accessions (Tables S4, S5) showed that the SNP at 4221 bp had little effect on phenotype variations (Figure S12). In contrast, the InDel at 5,048–5,095 bp (the C-terminal variation) was significantly associated with CT in 14 of 25 comparisons, and seedling SRs under severe and repeated DS (SR2 and SR3). Therefore, we assumed that C-terminal variation plays a crucial role in the drought tolerance of wheat. The CT and seedling SR of accessions with a 5,048–5,095-bp deletion were higher than those of accessions with the insertion (Figure 7A, B). Thus, the deletion allele at 5048–5095 bp represented the favorable allele for drought tolerance. To further validate the effect of the C-terminal variation of *TaPP2C158* on drought tolerance in wheat, the DH lines derived from a cross of Hanxuan 10 × Lumai 14 (Population 2) were used as the plant materials (Table S6). Similarly, the allele with 5,048–5,095-bp deletion had higher CT under 9 of 16 comparisons, and higher seedling SR than the allele with the insertion (Figure 7C, D). These results supported the notion that the C-terminal variations in the *TaPP2C158* affect CT and seedling SRs under drought.

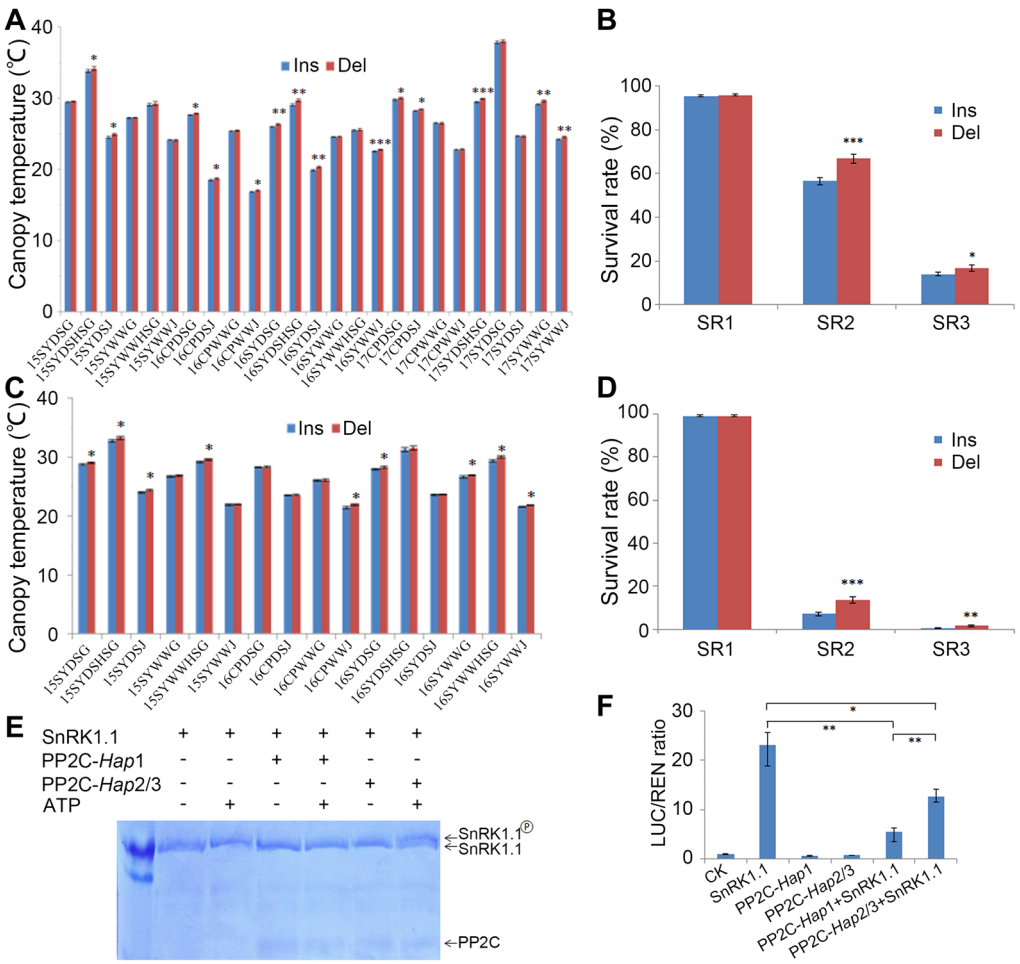

Figure 7. Genetic variations in *TaPP2C158* and their association with canopy temperature (CT), seedling survival rate (SR), and protein phosphatase activity

(A) Comparisons of CT in Population 1 (323 accessions) grown under 15 environments: planted in 2014–2015, 2015–2016, and 2016–2017 at Changping (CP) or Shunyi (SY), and under drought-stressed (DS) or well watered (WW) or heat-stressed (HS) conditions at the jointing (J) or grain-filling (G) stage. **(B)** Comparisons of seedling SRs in Population 1 (323 accessions) under three repeated DS. SR1 represents SRs under the first-time drought treatment (SR1), SR2 represents the second-time, and SR3 represents the third-time. **(C)** Comparisons of CT in Population 2 (doubled haploid) grown in 10 environments. **(D)** Comparisons of seedling SRs in Population 2 (doubled haploid) under three repeated DS. **(E)** Protein phosphatase activity difference of TaPP2C158 based on the InDel at 5,048–5,095 bp (C-terminal variation). Different forms of PP2C de-phosphorylated SnRK1.1 *in vitro*. Different forms of PP2C with His tagged were co-incubated with GST-tagged SnRK1.1 with or without ATP, and analyzed using Phos-tag mobility shift assays. Phosphorylated, non-phosphorylated SnRK1.1, and PP2C proteins are marked. **(F)** Expression of TaSnRK1.1-mediated *pTaRAB18:LUC* was significantly reduced by co-transformation with *PP2C-Hap*1 or *PP2C-Hap*2/3. *pTaRAB18:LUC* was co-transformed with *p35S:SnRK1.1* with or without *PP2C-Hap*1 or *PP2C-Hap*2/3 to the wheat protoplast. Luciferase activity was used to indicate the expression of the abscisic acid (ABA)-responsive gene *TaRAB18*, and REN was used as an internal control. Three independent experiments were performed with similar results. Data represent the means ± SE. *, *t*-test with $P < 0.05$. **, *t*-test with $P < 0.01$. ***, *t*-test with $P < 0.001$.

In order to clarify how C-terminal variations affect protein function, we compared the protein phosphatase activity of PP2C-*Hap*1 and PP2C-*Hap*2/3. The *PP2C-WT* was cloned from AK58, which is *Hap2*, so PP2C-WT has the same amino acid sequence as PP2C-*Hap2*/3. According to the method mentioned above, His-tagged PP2C-*Hap*1 was also expressed in *E. coli*. The de-phosphorylation activities of different alleles of TaPP2C158 protein forms against TaSnRK1.1 *in vitro* were checked. Phos-tagged SDS-PAGE showed that PP2C-*Hap*1 led to de-phosphorylation of TaSnRK1.1, while PP2C-*Hap2*/3 led to partial de-phosphorylation of TaSnRK1.1 (Figure 7E). Furthermore, luciferase assay using the *pTaRAB18:LUC* reporter was used to detect the effects of different *TaPP2C158* haplotypes on TaSnRK1.1-mediated *TaRAB18* expression in ABA signaling. LUC activity was reduced when *TaSnRK1.1* was co-transformed with *PP2C-Hap*1 or *PP2C-Hap*2/3. Moreover, the LUC activity of *PP2C-Hap*1 co-transformed with *TaSnRK1.1* was significantly lower than that of *PP2C-Hap*2/3 (Figure 7F). These results suggested that the allele of PP2C-*Hap2/3* had a weaker de-phosphorylation function compared with the allele PP2C-*Hap1*. Therefore, they may have a more robust response to ABA under DS, thus increasing CT and seedling SR under drought.

TaPP2C158 allele with drought tolerance was positively selected across different wheat production zones in China

Population 3 (157 landraces) and Population 4 (348 modern cultivars) covering 10 Chinese wheat production zones were used to investigate the geographical and temporal distribution of the *TaPP2C158* polymorphic site, the InDel at 5,048–5,095 bp. Alleles of 157 landraces and 348 modern cultivars are listed separately in Tables S7 and S8. The insertion allele was dominant in landraces across all 10 wheat production zones whereas, in modern cultivars, the frequency of the deletion allele increased in all 10 zones and became the dominant allele except in Zone X (Figure 8). As mentioned above, the allele with the deletion at 5,048–5,095 bp was the drought-tolerant allele. These results suggest that the favorable allele for drought tolerance has been positively selected in the history of wheat breeding in China.

DISCUSSION

Plant wilting under drought is a pivotal index of drought response. Three kinds of mutant genes could be identified by screening drought-induced wilting mutants. First, mutants with impaired water absorption, that is, abnormal root growth and/or development of these mutants, for example *dro1*, are able to absorb less water, resulting in leaf wilting. (Uga et al., 2013). Second, mutants with impaired water transport, as with *lew2*, cannot transport water smoothly to the leaves to maintain the transpiration demand, causing leaf wilting. (Chen et al., 2005). Third, mutants with high leaf transpiration rates that lose water rapidly and result in leaf wilting, for example *ost1* (Mustilli et al., 2002), *slac1* (Negi et al., 2008; Vahisalu et al., 2008), *ghr1* (Hua et al., 2012), and *los5/aba3* (Xiong et al., 2001). To date, we have identified a series of *drought-induced wilting* mutants of wheat. In this study, we demonstrated that a wheat mutant *diw1/TaPP2C158* is deficient in ABA-mediated stomatal closure, leading to leaf wilting.

In the present study, we found that *diw1* in wheat encoded a clade I serine/threonine protein phosphatase 2C (TaPP2C158; Figure S3). Reversible protein phosphorylation, a process executed by kinases and phosphatases, is crucial for the plant response to environmental stimuli. PP2Cs play a vital role in this process (Kong et al., 2015), and their activities are dynamically regulated (Hao et al., 2011b; Chen et al., 2021; Hsu et al., 2021). In many cases, PP2C activity is regulated by subdomain structures or association with other proteins, which could result in conformational changes, thereby leading to a switch between the active and inactive status (Bheri et al., 2021). For example, the *abil-1* mutation (Gly-180 to Asp) caused a significant reduction in the phosphatase activity of ABI1 (Bertauche et al., 1996). The Gly-168

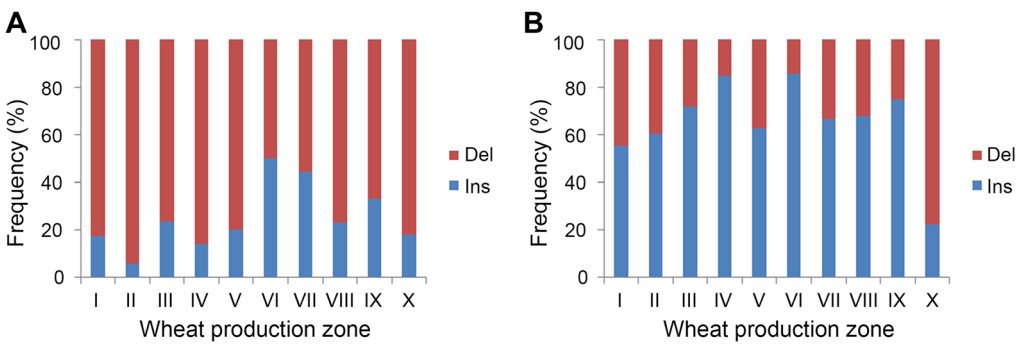

Figure 8. Frequency distribution of *TaPP2C158* alleles in 10 wheat production zones across China
Proportions of the two alleles in 157 Chinese landraces **(A)** and 348 modern cultivars **(B)**. I, Northern Winter Wheat Zone; II, Yellow and Huai River Valleys Facultative Wheat Zone; III, Middle and Low Yangtze Valleys Autumn-Sown Spring Wheat Zone; IV, Southwestern Autumn-Sown Spring Wheat Zone; V, Southern Autumn-Sown Spring Wheat Zone: VI, Northeastern Spring Wheat Zone; VII, Northern Spring Wheat Zone; VIII, Northwestern Spring Wheat Zone: IX, Qinghai-Tibetan Plateau Spring–Winter Wheat Zone; X, Xinjiang Winter–Spring Wheat Zone.

to Asp mutation reduced phosphatase activity in *abi2-1* (Leung et al., 1997; Merlot et al., 2001). EAR1 can bind to the N-terminal inhibition domain of PP2Cs and enhance the activity of PP2Cs (Sheen, 1998; Wang et al., 2018b). Many proteins, such as ABT (Wang et al., 2020), BIN2 (Wang et al., 2018a), FERONIA (Yu et al., 2012), RAF22 (Sun et al., 2022), ROP11 (Li et al., 2012), TMK1 (Yang et al., 2021), participate in regulating clade A PP2Cs activity. Our study showed that an amino acid change at the TaPP2C158 C-terminus increased PP2C activity, which differed from *abi1-1* and *abi2-1*, and the natural variations in its C-terminal 16 amino acids also led to differences in protein phosphatase activity. TaPP2C158-WT has a weaker de-phosphorylation function (Figure 5A), but a stronger downstream gene expression than TaPP2C158-MT (Figure 5L). Moreover, a similar relationship between TaPP2C158-*Hap*1 and TaPP2C158-*Hap2*/3 was found in the patterns of protein phosphatase activity and target downstream gene expression (Figure 7E, F). These results suggested that the C-terminaus of TaPP2C158 has a vital role in regulating enzyme activity, and TaPP2C158 protein phosphatase activity is negatively correlated with ABA signaling. Given that the expression of *TaPP2C158* was induced by DS and TaPP2C158 is a negative regulator, we expect that other proteins must be involved in down-regulating the activity of TaPP2C158 during DS, which may just like clade A PP2Cs that are induced by ABA and inhibited by ABA-bound PYLs (Park et al., 2009). However, the underlying mechanism needs to be further explored in future studies.

SnRK1s are a subfamily of serine/threonine kinases that act as central integrators in stress and energy signaling (Polge and Thomas, 2007). In *Arabidopsis*, SnRK1.1 and SnRK1.2 have been reported as the central integrators of a transcription network for linking stress and energy signaling (Baena-Gonzalez et al., 2007), while SnRK1.1 is also implicated in the sugar and ABA signaling pathways (Jossier et al., 2009; Zhang et al., 2008b). In wheat, ABA can enhance SnRK1 activity (Coello et al., 2012). In peas, SnRK1 can also coordinate metabolic and hormonal signals (Radchuk et al., 2010). Despite some proteins, such as protein phosphatase 5PTase13, clade E PP2C member PP2C74 and clade A PP2C member PP2CA, being found to interact with SnRK1s and both participating in the integration of multiple signaling pathways, forming a coordinated response (Ananieva et al., 2008; Tsugama et al., 2012; Rodrigues et al., 2013), the underlying molecular mechanisms in wheat are still poorly understood. In this study, through Y2H screening, we identified a TaPP2C158 interactor TaSnRK1.1, and found that TaSnRK1.1 was also involved in drought tolerance. Further studies have indicated that TaPP2C158 causes TaSnRK1.1 de-phosphorylation and inactivation, and that TaSnRK1.1 could phosphorylate TaAREB3. Hence, in wheat, the PP2C hub may regulate ABA signaling through TaSnRK1.1. The core ABA signaling pathway consisting of PYL–PP2C–SnRK2–AREB has been extensively studied in many plant species. However, TaPP2C158 cannot interact with TaPYL4 (Figure S7), and can phosphorylate TaSnRK1.1 but not TaSnRK2.10 (Figure S9), suggesting that TaPP2C158 is not involved in core ABA signaling, but in branching signaling via TaSnRK1.1.

Many studies have shown that natural variation in promoter regions affecting gene expression contributes to drought tolerance. For example, insertions in wheat *TaNAC071-A* and maize *ZmVPP1* promoters enhanced drought tolerance through drought-induced expression (Wang et al., 2016b; Mao et al., 2022b). Amino acid changes in the coding region of genes can also confer phenotypic adaptation to environments by altering protein activity (Mei et al., 2022). For example, FLOE1 is a tunable environmental sensor and its protein variation is involved in local adaptation (Dorone et al., 2021). The GS3 or OsMADS1 variant causes grain to be longer or more slender (Liu et al., 2018; Sun et al., 2018). In this study, we found a nucleotide change (G/A) in the exon 10 of *TraesCS5A02G359900* in the *diw1-1* mutant that resulted in a change in C-terminal amino acid (Ser364/Arg364), which in turn affected the protein phosphatase activity (Figure 2), leading to a change in drought tolerance-related phenotypes. The natural variation of the C-terminus also confers the difference in CT, seedling SR, and protein phosphatase activity (Figure 7).

Drought tolerance is a complex quantitative trait, inherently regulated by hundreds of genes. Although there are many evaluation criteria for drought tolerance, CT and SR under drought are effective indicators to distinguish drought-tolerant alleles (Wang et al., 2021a). In this study, 21 polymorphic sites of *TaPP2C158* were detected in the wheat germplasm, including a 48-bp InDel located in the C-terminal coding region, two synonymous SNPs, and 18 SNPs in the intron region (Figure 6A). However, only the InDel at 5048–5095 bp led to amino acid variation, which was significantly associated with CT and SR (Figure 7). The allele with 48-bp deletion exhibited stronger drought tolerance than that with the insertion. The SNP at 4221 bp in the intron region had no significant effect on phenotypic variation (Figure S12). In Chinese wheat, the frequency of the 5,048–5,095-bp deletion in TaPP2C158 increased from 20.0% in landraces to 65.8% in modern cultivars (Figure 8). This result demonstrated that the superior allele has been unconsciously positively selected by breeders during breeding, and suggests that it is important to explore and utilize the favorable alleles for improving drought tolerance of wheat.

In conclusion, we have identified a *diw1* mutant, in which a mutant gene (*TaPP2C158*) encodes a clade I protein phosphatase 2C, and found that TaPP2C158 coordinated with TaSnRK1.1 co-regulated ABA signaling. The C-terminal variation of TaPP2C158 resulted in differences in seedling SR under drought, CT, and protein phosphatase activity. *TaPP2C158* can serve as a direct target for genetic engineering, and its favorable haplotype (allele) is helpful for drought tolerance improvement in wheat.

MATERIALS AND METHODS

Wheat materials

Wheat (*Triticum aestivum* L.) mutants and the mapping population were used to evaluate drought tolerance and clone mutant genes. Transgenic wheat lines were constructed to character gene function. Four wheat populations, including three natural populations and a genetic population, were used for association analysis and allele spatiotemporal distribution. Specific wheat material information is presented as follows.

Growth conditions and physiological experiments

Drought tolerance evaluation of wheat accessions was carried out in a removable rain-off shelter at the Institute of Crop Sciences, Chinese Academy of Agricultural Sciences, as described previously (Li et al., 2018), during the spring in 2017–2021. In detail, the cultivation container (0.8 × 0.4 × 0.2 m, length × width × height) was filled with 20 kg of fluvo-aquic loam and buried in soil. Forty seeds per accession were sown, then the container was covered with 1 kg of soil. After emergence, 30 plants of each accession were reserved. The water loss of detached shoots of seedlings was measured at the three-leaf stage. Leaf rolling index and stomatal apertures were detected during the 2 weeks of water deprivation of plants, then phenotypes were photographed under drought conditions.

For water loss analysis, three seedling shoots were cut from plants and weighed at room temperature in 30% relative humidity at predetermined times. The water loss rate was calculated as the percentage of fresh weight lost. For the LRI assay, the maximum width (L_w) (approximately 1/3 location of the adaxial blade) and natural width (L_n) of the second fully extended leaf were measured at 9:00 a.m. to 10:30 a.m. LRI = $(L_w - L_n)/L_w \times 100\%$ (Fang et al., 2012). The stomatal aperture was measured by placing Arabic gum on the abaxial epidermis of the second fully extended leaf, obtaining images under a microscope, and using ImageJ software to measure the stomatal aperture. For ABA sensitivity in germination, wheat seeds were sown in Petri dishes with or without 20 μM ABA treatment. After incubation at 4°C for 2 d, germination percentages were counted based on visible radicle protrusion. For ABA sensitivity in primary root growth, wheat seeds were sown in Petri dishes with water and germinated at 4°C for 2 d and at room temperature for 2 d, then transferred to seed germination pouches with or without 30 μM ABA. After growth for 7 d, primary root length was measured.

Map-based cloning

Aikang 58 (AK58) is a high-yield dwarf wheat variety widely planted in China. AK58 mutants were induced by ethyl methanesulfonate. Zhongmai 36 (ZM36), a drought-tolerant and widely adaptable variety in China, was used as a hybrid parent. That is, the AK58 mutant *diw1-1* was crossed with ZM36 to obtain the F_2 population for selecting mutant plants based on wilting degree under drought. Using the bulked segregant analysis (BSA) method, two pools of extreme leaf-wilting types (30 mild wilting individuals and 30 severe wilting individuals) were constructed from individual plants from the F_2 population. The genotypes were detected with the Wheat 660K SNP array. Based on the CS simple sequence repeats (SSR) information on the website (http://202.194.139.32/PrimerServer/), in total, 150 SSR markers were developed in the 560–564 Mbp region of chromosome 5A, of which only 20 markers were polymorphic between the two parents AK58 and ZM36. After removing ~10% of seedlings with the false *diw1-1* phenotype based on their recombination at both markers 5A-97 and 5A-16, 2,859 *diw1-1* seedlings with the wilting phenotype were chosen from ~15,000 F_2 seedlings to map the *DIW1* gene. The primers used are listed in Table S9.

Production of transgenic wheat

For overexpression analysis, the coding sequence of *TaPP2C-MT* (*TaPP2C158* from *diw1-1*) was amplified and cloned into the pWMB110 vector that carries the ubiquitin promoter through seamless DNA cloning at the *Bam*HI site using the In-Fusion HD Cloning Plus kit. To analyze knockout mutants, we designed four primers for each of the *TaPP2C158* and *TaSnRK1.1* genes, which contained two 19-bp specific sequences of the corresponding genes, and then cloned pCBC-MT1T2 fragments into CRISPR/Cas9 vector pBUE414 with two guide RNAs targeting, separately. These constructs were introduced using *Agrobacterium tumefaciens* EHA105-mediated transformation into the immature embryos of bread wheat cv. Fielder according to established protocols (Ishida et al., 2015). Overexpressed transgenic T_1 and T_2 wheat seedlings were selected using the QuickStix Kit for PAT/*bar* (ENVIROLOGIX, USA). The wheat seedlings from 2-week-old homozygous T_3 lines were used to detect the expression of *TaPP2C158* through real-time PCR. *TaPP2C* or *TaSnRK1.1* knockout lines were analyzed by PCR and sequencing. Homozygous transgenic lines were selected for phenotypic observation. Primers P414A-R1/R2, P414B-F1/R1, P414D-F1/R1, SnRKA-F1/R1, SnRKB-F1/R1, and SnRKD-F1/R1, were used to detect the genome specificity of the mutant sites. The primers used are listed in Table S9.

TaPP2C158 gene expression analysis

Root and leaf tissues from wheat cv. Hanxuan 10 growing in deionized water and from 2-week-old seedlings and different tissues at the flowering stage (root, stem, flag leaf, and spike) were sampled for spatiotemporal expression pattern analysis. Two-week-old wheat plants growing in deionized water were sprayed with 50 μM ABA solution, and whole seedlings were harvested at 0, 1, 3, 6, and 12 h after treatment. Total RNA was extracted, and real-time PCR analysis was carried out. The *TaGAPDH* gene was used as an internal control to normalize the data. Three biological replicates and three technical replicates were performed.

TaPP2C-MT overexpression lines from 2-week-old seedlings were harvested to analyze the expression of the *TaPP2C158* gene. Total RNA was extracted and reversely transcribed into cDNA, and then analyzed by real-time PCR. The *Tubulin* gene was used as an internal control to normalize the data. The primers used are listed in Table S9.

Phylogenetic analysis

The amino acid sequences of PP2C158 from different species were identified from the NCBI database using the BLAST algorithm. Based on the full-length amino acid sequences, phylogenetic analysis was performed using Molecular Evolutionary Genetics Analysis (MEGA) software version 5.2 and the neighbor-joining method with 1000 bootstrap sampling.

Subcellular localization

The *TaPP2C158* cDNA PCR products were fused into a modified vector pCAMBIA1300, which contained a super promoter and GFP cDNA, through seamless DNA cloning at the *Xba*I and *Kpn*I sites using the In-Fusion® HD Cloning Plus kit, then transformed into *Agrobacterium* GV3101 and injected into *N. benthamiana* leaves. The plants were grown in a greenhouse for 48 h, then the GFP signal was detected under a Zeiss LSM700 confocal laser-scanning microscope. At the same time, the constructs were also transformed into wheat protoplasts to detect their subcellular localization, as previously described (Wang et al., 2021b). The primers used are listed in Table S9.

TaPP2C158 Y2H screening and Y2H assay

The *TaPP2C158* full-length coding sequence was amplified from AK58 cDNA, fused into pGBKT7 vector, through seamless DNA cloning at the *Bam*HI site using the In-Fusion® HD Cloning Plus kit, and transformed into yeast strain Y2H as bait. A cDNA library in yeast strain Y187 derived from stress-treated wheat seedlings was used in this experiment (Wang et al., 2019a). Yeast-two-hybrid screening was performed according to the manufacturer's protocol (Clontech, USA). In brief, after mating, the culture was plated onto SD agar plates lacking Leu, Trp, His, and Ura, but containing X-α-Gal, then incubated for 4 d at 30°C. Blue colonies with good growth were selected for sequencing. By sequencing 1248 clones, 480 fragments were obtained, 297 fused sequences were acquired, and 45 genes were finally detected. Among them, six clones were identified as TaSnRK1.1, coding from the 332 a.a. to the 503 a.a. (C-terminaus) of TaSnRK1.1.

For Y2H assays, the *TaSnRK1.1* full-length coding sequence was amplified from AK58 cDNA, and fused into the pGADT7 vector through seamless DNA cloning at a the *Bam*HI site using the In-Fusion® HD Cloning Plus kit. Then pGBKT7 with *TaPP2C158* and pGADT7 with *TaSnRK1.1* plasmids were co-transformed into yeast strain AH109 according to the manufacturer's protocol using the PEG/LiAc method (Clontech). The primers used are listed in Table S9.

Bimolecular fluorescence complementation assay

The full-length coding sequences of *TaPP2C158* and *TaSnRK1.1* were cloned into the YCE or YNE vector at the *Pac*I and *Spe*I restriction enzyme sites, through seamless DNA cloning, and transformed into *Agrobacterium tumefaciens* strain GV3101. The different combinations were mixed and injected into *N. benthamiana* leaves, and the plants were cultured for 48 h, then YFP signals were detected under a confocal laser-scanning microscope (Zeiss LSM700; Germany). The primers used are listed in Table S9.

Firefly LCI assay

The full-length coding sequence of *TaPP2C158* was cloned into the cLUC vector at the *Kpn*I and *Bam*HI restriction enzyme sites, while *TaSnRK1.1* was cloned into nLUC at the *Kpn*I and *Sal*I sites, and transformed into *Agrobacterium tumefaciens* strain GV3101. Different combinations were mixed and injected into *N. benthamiana* leave, and the plants were cultured for 48 h. After 1 mM luciferin was sprayed onto the leaves in the dark for 5 min, the LUC image was captured using a low-light-cooled charge-coupled device (CCD) imaging device (NightSHADE, Germany) with Indigo software. Primers are listed in Table S9.

Co-immunoprecipitation assay

The full-length coding sequences (CDS) of *TaSnRK1.1* were fused into the pCAMBIA1300 vector, which contains a super promoter and Flag-tag, through seamless DNA cloning at the *Xba*I and *Sal*I sites, and transformed into *Agrobacterium tumefaciens* strain GV3101. Different combinations with GFP and/or Flag-tag were mixed and injected into *N. benthamiana* leaves, and the plants were cultured for 48 h. Total proteins were extracted using lysis buffer (50 mM Tris-HCl (pH 7.5), 150 mM NaCl, 0.1% Triton X-100) with freshly added 10 mM phenylmethylsulfonyl fluoride (PMSF), protease inhibitor cocktail (Roche, Switzerland). Extracts were then clarified by centrifugation at 4°C for 5 min. Then supernatants were mixed with 50 μL anti-GFP mAb-magnetic beads (MBL, Japan) for 1 h with gentle rotation at 4°C, and subsequently the beads were washed three times with lysis buffer, and boiled for 5 min. After centrifugation, the supernatants were used for immune-blotting analysis with 1:5000 anti-Flag (MBL, Japan) antibody or 1:1,000 anti-GFP (Roche) antibody and 1:5,000 HRP goat anti-mouse IgG (Abbkine, China). The primers used are listed in Table S9.

Recombinant protein expression and purification

The *TaPP2C158* full-length coding sequences *PP2C-WT* and *PP2C-MT* were amplified from AK58 and mutant cDNA separately, and fused into the pET30a vector containing the His tag through seamless DNA cloning at the *Bam*HI restriction site. Proteins were expressed in BL21 strains with 0.5 mM IPTG for 8 h at 37°C, 200 r/min. The culture was then collected by centrifugation at 6,000 *g* for 10 min at 4°C, resuspended in PBS (with PMSF and cocktail) and sonicated for 10 min. After centrifugation, the supernatant was incubated with ProteinIso Ni-NTA Resin (TRANS, China) for 2 h

at 4°C. After washing three times with PBS, the proteins were eluted from the resin with elution buffer (50 mM NaH_2PO_4, 30 mM NaCl, and 250 mM imidazole, pH 7.4).

The *TaSnRK1.1* full-length coding sequence was amplified from AK58 cDNA, and fused into the pGEX-4T1 vector containing the GST tag, through seamless DNA cloning at an *Eco*RI site. Proteins were expressed in Transetta strains using 0.5 mM IPTG for 8 h at 16°C, 75 r/min. The culture was then collected by centrifugation at 6000 *g* for 10 min at 4°C, re-suspended in PBS (with PMSF and cocktail) and sonicated for 10 min. After centrifugation, the supernatant was incubated with Glutathione Resin (GenScript, China) for 2 h at 4°C. After washing three times with PBS, the proteins were eluted from the resin using glutathione (GSH) buffer (50 mM Tris-HCl, pH 8.0, and 10 mM GSH). The purified protein concentration was measured at 595 nm with Quick Start Bradford Dye Reagent (Bio-Rad, USA), while using BSA as a standard curve. The primers used are listed in Table S9.

The cDNA of *TaAREB3* was fused to pGEX-4T1 with a GST tag, and its protein was expressed and purified as described previously (Wang et al., 2016a). The *TaSnRK2.10* full-length CDS was fused into the pMAL vector containing the MBP tag (Zhang et al., 2023). Protein was expressed and purified with Amylose Resin (NEB, USA).

Measurement of TaPP2C activity

TaPP2C158 activity was measured using a Ser/Thr Phosphatase Assay Kit (Promega, USA) as described previously (Wang et al., 2018b). In brief, His-tagged TaPP2C-WT and TaPP2C-MT were expressed and purified in *E. coli* as described PREVIOUSLY. None of the buffers used for this experiment contained phosphate. To measure phosphatase activity, different concentrations of PP2C proteins were mixed in a 50-μL volume with 5 μL of 1 mM phosphopeptide and 10 μL of PP2C 5× reaction buffer at 25°C for 15 min. The reactions were stopped by adding 50 μL molybdate dye/additive mixtures. The plate was incubated at room temperature for 15 min, then the absorbance was measured at 630 nm. The primers used are listed in Table S9.

To measure the total TaPP2C activity in plants, total proteins (0.1 g) from the wild-type and mutant were extracted in phosphatase storage buffer also as described previously by Wang et al. (2018b). In brief, after samples were homogenized, the lysate was centrifuged at 100,000 *g* for 60 min at 4°C, then Sephadex G-25 resin was used to remove the endogenous phosphates in the tissue extract. The protein concentration of the filtered lysate was measured, and the PP2C activity of the lysate was determined by the above method with the addition of 5 mM okadaic acid.

In vitro phosphorylation assay and Phos-tag mobility shift assay

In vitro phosphorylation assays were performed as previously described (Han et al., 2020). Wild-type or mutated TaPP2C158 protein fused with a His tag were co-incubated with GST-tagged TaSnRK1.1 proteins in a total volume of 30 μL of kinase reaction buffer with or without ATP at 30°C for 60 min. The reaction was stopped by adding one volume of 2× SDS sample loading buffer. After boiling at 95°C for 5 min, proteins were separated on Phos-tag acrylamide gel. The Phos-tag mobility shift assays were performed according to the manufacturer's instructions (Wako, Japan) on 8% Phos-tag gels with 100 mM Phos-tag and 100 mM $MnCl_2$, followed by Coomassie brilliant blue R250 staining. TaPP2C158 was co-incubated with TaSnRK1.1 or TaSnRK2.10 for *in vitro* phosphorylation assays as described previously. TaSnRK1.1 and TaAREB3 were also co-incubated for *in vitro* phosphorylation assays as described previously.

In vivo phosphorylation assay

An empty pCAMBIA1300 vector containing Flag-tag and pCAMBIA1300 vector fused with *TaSnRK1.1* and Flag-tag were extracted using the Plasmid Maxprep Kit (Vigorous, UK). The constructs were transformed into wild-type Fielder and *diw1-2* wheat protoplasts, separately, as previously described (Wang et al., 2021b). Phos-tag mobility shift assay and immune-blotting analysis were performed as described previously.

After centrifugation, the supernatants were used for immunoblotting analysis with 1:5,000 anti-Flag (MBL, Japan) antibody or 1:1,000 anti-GFP (Roche) antibody and 1:5,000 HRP goat anti-mouse IgG (Abbkine, China).

Luciferase assay of transformed wheat protoplasts

Wheat protoplast transient expression was performed as previously described (Yoo et al., 2007; Wang et al., 2021b). The *TaRAB18* promoter fragment (−548 to −7 bp) was amplified and ligated into the vector pGreen II 0800-LUC through seamless DNA cloning at the *Hin*dIII and *Nco*I sites. Together with *PP2C-WT*, *PP2C-MT*, and/or *SnRK1.1* in the pCAMBIA1300 vector, this construct was co-transformed into the wheat protoplast. The activities of firefly luciferase (LUC) and Renilla luciferase (REN) were measured using the Dual-Glo® Luciferase Assay System (Promega, USA) with a multimode reader at 48 h after transformation. The activity was calculated as the ratio of LUC to REN, and the ratio in leaves transformed with the empty vector (pCAMBIA1300/pGreen II 0800-LUC) was set to 1. In addition, different *TaPP2C158* haplotypes and/or *SnRK1.1* in the pCAMBIA1300 *pTaRAB18:LUC* reporter vector were co-transformed into the wheat protoplast, and the luciferase assay was performed as described previously. The primers used are listed in Table S9.

Four wheat populations

The *TaPP2C158* gene was amplified and sequenced from a panel of 32 highly diverse wheat accessions that were screened with 209 SSR markers (Zhang et al., 2013), then the nucleotide polymorphism was analyzed. Four wheat populations were used for different purposes. Population 1, comprised of 323 wheat accessions, including 209 modern cultivars, 43 advanced lines, and 10 landraces, was used for association analysis (Wang et al., 2021b). Population 2, a doubled-haploid (DH) genetic population consisting of 150 lines derived from the cross

Hanxuan10 × Lumai14, was used for verifying the phenotypes of different alleles (Wang et al., 2019b). Population 3 consisted of 157 landraces, and Population 4 consisted of 348 modern cultivars, from a Chinese wheat mini-core collection (Hao et al., 2011a), and were used to determine the geographical and temporal distribution of different wheat alleles in China.

Seedling SR evaluation of the wheat panels under drought

The evaluation of seedling SR under drought conditions was carried out in a removable rain-off shelter at the Institute of Crop Sciences, Chinese Academy of Agricultural Sciences with three replicates, and as described previously (Li et al., 2018). The wheat Population 1 was phenotyped in the spring of 2015, Population 2 in 2007, and overexpression and mutant lines during 2019-2021. Briefly, 21 accessions each of 40 seeds were sown in a cultivation container (0.8 × 0.4 × 0.2 m, length × width × height), which was covered with 1 kg of soil after sowing. After emergence, 30 plants are reserved for each accession. Seedlings at the three-leaf stage were subjected to the first drought. The soil water content at the beginning of drought treatment was ~22.0%. At ~10 d of no-watering treatment, the soil water content decreased to ~4.0%, and 2.0 L water was added to each container. The first SR (SR1) of each accession seedlings was investigated on the 5th d after re-watering. After another 15 d of the second drought treatment and re-watering, the second SR (SR2) of the seedlings was investigated. The third SR (SR3) of the seedlings was investigated after repeated water treatments.

Measurement of CT

Canopy temperatures at the jointing stage and grain-filling stage were detected as described previously (Li et al., 2019). Briefly, Population 1 was planted in 15 environments (year × site × water regime × heat combinations) at Shunyi (40°23′ N, 116°56′ E) and Changping (40°13′ N, 116°13′ E) in Beijing in three growing seasons: 2014–2015, 2015-2016, and 2016-2017. Population 2 was planted in 10 environments (year × site × water regime × heat stress combinations), including the same sites as Population 1 in two growing seasons: 2014-2015 and 2015-2016. Two water regimes were applied, that is well watered (WW) plots were irrigated with 750 m^3 ha^{-1} (75 mm) water at pre-overwintering, flowering, and grain filling when the amounts of rainfall were insufficient, whereas DS plots were rain fed only. The amounts of rainfall during the three growing seasons were 161, 173, and 143 mm. Heat-stress (HS) treatment was applied at 1 week of post-anthesis at Shunyi by placing a plastic sheet over steel frames in the field.

Yield-related phenotypic analysis of mutants and transgenic lines

Plants were grown in fields containing a removable rain-off shelter (DS) and the corresponding WW plots, as 1 m single row plots spaced 30 cm apart, and with 10 plants per row with normal field management in two growing seasons, 2019-2020 and 2020-2021. The amounts of rainfall during the growing seasons were 161 and 193 mm. Spike number per plant, grain number per spike, and 1000-grain weight were recorded post-harvest.

Marker development

A dCAPS marker was developed based on a SNP (T/C) at position 4,221 bp, which contained a mismatched nucleotide to produce a restriction enzyme site for *Ava*II. Genome-specific primers (PP2C-5A-F2/R2) were used to obtain the first-round PCR product, which was used as the template for the second round of PCR. Last, the PCR products were digested with restriction enzymes and separated by electrophoresis on a 4% agarose gel. In addition, a PCR marker was developed based on the 48-bp InDel at 5,048–5,095 bp. The PCR products were amplified and separated on a 2.5% gel. The primers used are listed in Table S9.

Association analysis

Association analysis between phenotype and genotype was mainly performed as described previously (Li et al., 2019). Briefly, the structure of Population 1 was detected using STRUCTURE 2.3.4 software. The mix linear model (MLM) in TASSEL (version 5.2.51) software was applied with the population structure (*Q*) as the covariant. A *P*-value < 0.05 was considered to show a significant difference. Analysis of variance using SPSS (version 19.0) software was used to detect the effects of two polymorphic sites on CT and seedling SR.

Gene IDs

Sequence data from this article can be found in the WheatOmics data libraries under the following Gene ID: *TaPP2C158*, *TraesCS5A02G359900*; *TaSnRK1.1*, *TraesCS1A02G350500*; *TaAREB3*, *TraesCS3B01G368300*; *TaRAB18*, *TraesCS5A02G369800*; *TaPYL4*, *TraesCS2A02G089400*; and *TaSnRK2.10*, *TraesCS4B02G079300*.

ACKNOWLEDGEMENTS

The authors thank Dr. Zhizhong Gong (Chinese Agricultural University) for giving constructive suggestions; Dr. Mingming Xin (Chinese Agricultural University) for providing the CRISPR-Cas9 vector to generate *TaPP2C158* mutant (*diw1-2*) and *TaSnRK1.1* mutant; and Professor Genying Li (Shandong Academy of Agricultural Sciences, China) for helping us to get transgenic wheat lines. This work was funded by the National Natural Science Foundation of China (32061143040), the Agricultural Science and Technology Innovation Program (ZDRW202002), and the Central Public-interest Scientific Institution Basal Research Fund (Y2022GH06).

CONFLICTS OF INTEREST

The authors declare no conflict of interest.

AUTHOR CONTRIBUTION

J.W. and R.J. conceived and designed the experiments; J.W. completed the main work of plant material cultivation, result investigation, and wrote the original draft; C.L. took part in detecting protein interaction; L.L. participated in the association analysis; L.G. and J.J. built AK58 mutant libraries; G.H. performed map-based cloning; Y.Z. expressed and purified recombination protein; X.Z. provided wheat Populations 3 and 4; M.P.R. and X.M. revised the manuscript and gave constructive comments; R.J. supervised the experiments and revised the manuscript. All authors discussed the results and provided feedback on the manuscript.

Edited by: Pengcheng Wang, Southern University of Science and Technology, China

Received Jan. 13, 2023; **Accepted** May 8, 2023; **Published** May 9, 2023

OO: OnlineOpen

REFERENCES

Ananieva, E.A., Gillaspy, G.E., Ely, A., Burnette, R.N., and Erickson, F. L. (2008). Interaction of the WD40 domain of a myoinositol polyphosphate 5-phosphatase with SnRK1 links inositol, sugar, and stress signaling. Plant Physiol. **148:** 1868–1882.

Baena-Gonzalez, E., Rolland, F., Thevelein, J.M., and Sheen, J. (2007). A central integrator of transcription networks in plant stress and energy signalling. Nature **448:** 938–942.

Bertauche, N., Leung, J., and Giraudat, J. (1996). Protein phosphatase activity of abscisic acid insensitive 1 (ABI1) protein from *Arabidopsis thaliana*. Eur. J. Biochem. **241:** 193–200.

Bheri, M., Mahiwal, S., Sanyal, S.K., and Pandey, G.K. (2021). Plant protein phosphatases: What do we know about their mechanism of action? FEBS J. **288:** 756–785.

Brandt, B., Brodsky, D.E., Xue, S., Negi, J., Iba, K., Kangasjarvi, J., Ghassemian, M., Stephan, A.B., Hu, H., and Schroeder, J.I. (2012). Reconstitution of abscisic acid activation of SLAC1 anion channel by CPK6 and OST1 kinases and branched ABI1 PP2C phosphatase action. Proc. Natl. Acad. Sci. U.S.A. **109:** 10593–10598.

Chen, X., Ding, Y., Yang, Y., Song, C., Wang, B., Yang, S., Guo, Y., and Gong, Z. (2021). Protein kinases in plant responses to drought, salt, and cold stress. J. Integr. Plant Biol. **63:** 53–78.

Chen, Z., Hong, X., Zhang, H., Wang, Y., Li, X., Zhu, J.K., and Gong, Z. (2005). Disruption of the cellulose synthase gene, *AtCesA8/IRX1*, enhances drought and osmotic stress tolerance in *Arabidopsis*. Plant J. **43:** 273–283.

Coello, P., Hirano, E., Hey, S.J., Muttucumaru, N., Martinez-Barajas, E., Parry, M.A., and Halford, N.G. (2012). Evidence that abscisic acid promotes degradation of SNF1-related protein kinase (SnRK) 1 in wheat and activation of a putative calcium-dependent SnRK2. J. Exp. Bot. **63:** 913–924.

Cutler, S.R., Rodriguez, P.L., Finkelstein, R.R., and Abrams, S.R. (2010). Abscisic acid: Emergence of a core signaling network. Annu. Rev. Plant Biol. **61:** 651–679.

Dorone, Y., Boeynaems, S., Flores, E., Jin, B., Hateley, S., Bossi, F., Lazarus, E., Pennington, J.G., Michiels, E., De Decker, M., et al. (2021). A prion-like protein regulator of seed germination undergoes hydration-dependent phase separation. Cell **184:** 4284–4298.

Fabregas, N., Yoshida, T., and Fernie, A.R. (2020). Role of Raf-like kinases in SnRK2 activation and osmotic stress response in plants. Nat. Commun. **11:** 6184.

Fang, L., Zhao, F., Cong, Y., Sang, X., Du, Q., Wang, D., Li, Y., Ling, Y., Yang, Z., and He, G. (2012). Rolling-leaf14 is a 2OG-Fe (II) oxygenase family protein that modulates rice leaf rolling by affecting secondary cell wall formation in leaves. Plant Biotechnol. J. **10:** 524–532.

Fleury, D., Jefferies, S., Kuchel, H., and Langridge, P. (2010). Genetic and genomic tools to improve drought tolerance in wheat. J. Exp. Bot. **61:** 3211–3222.

Fujii, H., Chinnusamy, V., Rodrigues, A., Rubio, S., Antoni, R., Park, S. Y., Cutler, S.R., Sheen, J., Rodriguez, P.L., and Zhu, J.K. (2009). *In vitro* reconstitution of an abscisic acid signalling pathway. Nature **462:** 660–664.

Gahlaut, V., Jaiswal, V., Tyagi, B.S., Singh, G., Sareen, S., Balyan, H.S., and Gupta, P.K. (2017). QTL mapping for nine drought-responsive agronomic traits in bread wheat under irrigated and rain-fed environments. PLoS ONE **12:** e0182857.

Gong, Z., Xiong, L., Shi, H., Yang, S., Herrera-Estrella, L.R., Xu, G., Chao, D. Y., Li, J., Wang, P.Y., Qin, F., et al. (2020). Plant abiotic stress response and nutrient use efficiency. Sci. China: Life Sci. **63:** 635–674.

Guo, Y., Shi, Y., Wang, Y., Liu, F., Li, Z., Qi, J., Wang, Y., Zhang, J., Yang, S., Wang, Y., et al. (2022). The clade F PP2C phosphatase ZmPP84 negatively regulates drought tolerance by repressing stomatal closure in maize. New Phytol. **237:** 1728–1744.

Han, X., Zhang, L., Zhao, L., Xue, P., Qi, T., Zhang, C., Yuan, H., Zhou, L., Wang, D., Qiu, J., et al. (2020). SnRK1 phosphorylates and destabilizes WRKY3 to enhance barley immunity to powdery mildew. Plant Commun. **1:** 100083.

Hao, C., Wang, L., Ge, H., Dong, Y., and Zhang, X. (2011a). Genetic diversity and linkage disequilibrium in Chinese bread wheat (*Triticum aestivum* L.) revealed by SSR markers. PLoS ONE **6:** e17279.

Hao, Q., Yin, P., Li, W., Wang, L., Yan, C., Lin, Z., Wu, J.Z., Wang, J., Yan, S.F., and Yan, N. (2011b). The molecular basis of ABA-independent inhibition of PP2Cs by a subclass of PYL proteins. Mol. Cell **42:** 662–672.

Hsu, P.K., Dubeaux, G., Takahashi, Y., and Schroeder, J.I. (2021). Signaling mechanisms in abscisic acid-mediated stomatal closure. Plant J. **105:** 307–321.

Hua, D., Wang, C., He, J., Liao, H., Duan, Y., Zhu, Z., Guo, Y., Chen, Z., and Gong, Z. (2012). A plasma membrane receptor kinase, GHR1, mediates abscisic acid- and hydrogen peroxide-regulated stomatal movement in *Arabidopsis*. Plant Cell **24:** 2546–2561.

Ishida, Y., Tsunashima, M., Hiei, Y., and Komari, T. (2015). Wheat (*Triticum aestivum* L.) transformation using immature embryos. Methods Mol. Biol. **1223:** 189–198.

Jossier, M., Bouly, J.P., Meimoun, P., Arjmand, A., Lessard, P., Hawley, S., Grahame Hardie, D., and Thomas, M. (2009). SnRK1 (SNF1-related kinase 1) has a central role in sugar and ABA signalling in *Arabidopsis thaliana*. Plant J. **59:** 316–328.

Katsuta, S., Masuda, G., Bak, H., Shinozawa, A., Kamiyama, Y., Umezawa, T., Takezawa, D., Yotsui, I., Taji, T., and Sakata, Y. (2020). *Arabidopsis* Raf-like kinases act as positive regulators of subclass III SnRK2 in osmostress signaling. Plant J. **103:** 634–644.

Kong, L., Cheng, J., Zhu, Y., Ding, Y., Meng, J., Chen, Z., Xie, Q., Guo, Y., Li, J., Yang, S., et al. (2015). Degradation of the ABA co-receptor ABI1 by PUB12/13 U-box E3 ligases. Nat. Commun. **6:** 8630.

Lesk, C., Rowhani, P., and Ramankutty, N. (2016). Influence of extreme weather disasters on global crop production. Nature **529:** 84–87.

Leung, J., Merlot, S., and Giraudat, J. (1997). The *Arabidopsis ABSCISIC ACID-INSENSITIVE2* (*ABI2*) and *ABI1* genes encode homologous protein phosphatases 2C involved in abscisic acid signal transduction. Plant Cell **9:** 759–771.

Li, L., Mao, X., Wang, J., Chang, X., Liu, Y., and Jing, R. (2018). Drought tolerance evaluation of wheat germplasm resources. Acta Agron. Sin. **44:** 988–999.

Li, L., Peng, Z., Mao, X., Wang, J., Chang, X., Reynolds, M., and Jing, R. (2019). Genome-wide association study reveals genomic regions controlling root and shoot traits at late growth stages in wheat. Ann. Bot. **124:** 993–1006.

Li, S., Yu, S., Zhang, Y., Zhu, D., Li, F., Chen, B., Mei, F., Du, L., Ding, L., Chen, L., et al. (2022). Genome-wide association study revealed *TaHXK3-2A* as a candidate gene controlling stomatal index in wheat seedlings. Plant Cell Environ. **45:** 2306–2323.

Li, Z., Li, Z., Gao, X., Chinnusamy, V., Bressan, R., Wang, Z.X., Zhu, J. K., Wu, J.W., and Liu, D. (2012). ROP11 GTPase negatively regulates ABA signaling by protecting ABI1 phosphatase activity from inhibition by the ABA receptor RCAR1/PYL9 in *Arabidopsis*. J. Integr. Plant Biol. **54:** 180–188.

Lin, C.R., Lee, K.W., Chen, C.Y., Hong, Y.F., Chen, J.L., Lu, C.A., Chen, K.T., Ho, T.H., and Yu, S.M. (2014). SnRK1A-interacting negative regulators modulate the nutrient starvation signaling sensor SnRK1 in source-sink communication in cereal seedlings under abiotic stress. Plant Cell **26:** 808–827.

Lin, Z., Li, Y., Zhang, Z., Liu, X., Hsu, C.C., Du, Y., Sang, T., Zhu, C., Wang, Y., Satheesh, V., et al. (2020). A RAF-SnRK2 kinase cascade mediates early osmotic stress signaling in higher plants. Nat. Commun. **11:** 613.

Liu, Q., Han, R., Wu, K., Zhang, J., Ye, Y., Wang, S., Chen, J., Pan, Y., Li, Q., Xu, X., et al. (2018). G-protein betagamma subunits determine grain size through interaction with MADS-domain transcription factors in rice. Nat. Commun. **9:** 852.

Ma, Y., Szostkiewicz, I., Korte, A., Moes, D., Yang, Y., Christmann, A., and Grill, E. (2009). Regulators of PP2C phosphatase activity function as abscisic acid sensors. Science **324:** 1064–1068.

Mao, H., Jian, C., Cheng, X., Chen, B., Mei, F., Li, F., Zhang, Y., Li, S., Du, L., Li, T., et al. (2022a). The wheat ABA receptor gene *TaPYL1-1B* contributes to drought tolerance and grain yield by increasing water-use efficiency. Plant Biotechnol. J. **20:** 846–861.

Mao, H., Li, S., Chen, B., Jian, C., Mei, F., Zhang, Y., Li, F., Chen, N., Li, T., Du, L., et al. (2022b). Variation in *cis*-regulation of a NAC transcription factor contributes to drought tolerance in wheat. Mol. Plant **15:** 276–292.

Mao, H., Li, S., Wang, Z., Cheng, X., Li, F., Mei, F., Chen, N., and Kang, Z. (2020). Regulatory changes in *TaSNAC8-6A* are associated with drought tolerance in wheat seedlings. Plant Biotechnol. J. **18:** 1078–1092.

Mega, R., Abe, F., Kim, J.S., Tsuboi, Y., Tanaka, K., Kobayashi, H., Sakata, Y., Hanada, K., Tsujimoto, H., Kikuchi, J., et al. (2019). Tuning water-use efficiency and drought tolerance in wheat using abscisic acid receptors. Nat. Plants **5:** 153–159.

Mei, F., Chen, B., Du, L., Li, S., Zhu, D., Chen, N., Zhang, Y., Li, F., Wang, Z., Cheng, X., et al. (2022). A gain-of-function allele of a DREB transcription factor gene ameliorates drought tolerance in wheat. Plant Cell **34:** 4472–4494.

Melcher, K., Ng, L.M., Zhou, X.E., Soon, F.F., Xu, Y., Suino-Powell, K. M., Park, S.Y., Weiner, J.J., Fujii, H., Chinnusamy, V., et al. (2009). A gate-latch-lock mechanism for hormone signalling by abscisic acid receptors. Nature **462:** 602–608.

Merlot, S., Gosti, F., Guerrier, D., Vavasseur, A., and Giraudat, J. (2001). The ABI1 and ABI2 protein phosphatases 2C act in a negative feedback regulatory loop of the abscisic acid signalling pathway. Plant J. **25:** 295–303.

Mustilli, A.C., Merlot, S., Vavasseur, A., Fenzi, F., and Giraudat, J. (2002). *Arabidopsis* OST1 protein kinase mediates the regulation of stomatal aperture by abscisic acid and acts upstream of reactive oxygen species production. Plant Cell **14:** 3089–3099.

Negi, J., Matsuda, O., Nagasawa, T., Oba, Y., Takahashi, H., Kawai-Yamada, M., Uchimiya, H., Hashimoto, M., and Iba, K. (2008). CO_2 regulator SLAC1 and its homologues are essential for anion homeostasis in plant cells. Nature **452:** 483–486.

Park, S.Y., Fung, P., Nishimura, N., Jensen, D.R., Fujii, H., Zhao, Y., Lumba, S., Santiago, J., Rodrigues, A., Chow, T.F., et al. (2009). Abscisic acid inhibits type 2C protein phosphatases via the PYR/PYL family of START proteins. Science **324:** 1068–1071.

Park, S.Y., Peterson, F.C., Mosquna, A., Yao, J., Volkman, B.F., and Cutler, S.R. (2015). Agrochemical control of plant water use using engineered abscisic acid receptors. Nature **520:** 545–548.

Polge, C., and Thomas, M. (2007). SNF1/AMPK/SnRK1 kinases, global regulators at the heart of energy control? Trends Plant Sci. **12:** 20–28.

Radchuk, R., Emery, R.J., Weier, D., Vigeolas, H., Geigenberger, P., Lunn, J.E., Feil, R., Weschke, W., and Weber, H. (2010). Sucrose non-fermenting kinase 1 (SnRK1) coordinates metabolic and hormonal signals during pea cotyledon growth and differentiation. Plant J. **61:** 324–338.

Rodrigues, A., Adamo, M., Crozet, P., Margalha, L., Confraria, A., Martinho, C., Elias, A., Rabissi, A., Lumbreras, V., Gonzalez-Guzman, M., et al. (2013). ABI1 and PP2CA phosphatases are negative regulators of Snf1-related protein kinase1 signaling in *Arabidopsis*. Plant Cell **25:** 3871–3884.

Santiago, J., Dupeux, F., Round, A., Antoni, R., Park, S.Y., Jamin, M., Cutler, S.R., Rodriguez, P.L., and Marquez, J.A. (2009). The abscisic acid receptor PYR1 in complex with abscisic acid. Nature **462:** 665–668.

Sheen, J. (1998). Mutational analysis of protein phosphatase 2C involved in abscisic acid signal transduction in higher plants. Proc. Natl. Acad. Sci. U.S.A. **95:** 975–980.

Shiferaw, B., Smale, M., Braun, H.J., Duveiller, E., Reynolds, M., and Muricho, G. (2013). Crops that feed the world 10. Past successes and future challenges to the role played by wheat in global food security. Food Secur. **5:** 291–317.

Soon, F.F., Ng, L.M., Zhou, X.E., West, G.M., Kovach, A., Tan, M.H., Suino-Powell, K.M., He, Y., Xu, Y., Chalmers, M.J., et al. (2012). Molecular mimicry regulates ABA signaling by SnRK2 kinases and PP2C phosphatases. Science **335:** 85–88.

Sun, S., Wang, L., Mao, H., Shao, L., Li, X., Xiao, J., Ouyang, Y., and Zhang, Q. (2018). A G-protein pathway determines grain size in rice. Nat. Commun. **9:** 851.

Sun, Z., Feng, Z., Ding, Y., Qi, Y., Jiang, S., Li, Z., Wang, Y., Qi, J., Song, C., Yang, S., et al. (2022). RAF22, ABI1 and OST1 form a dynamic interactive network that optimizes plant growth and responses to drought stress in Arabidopsis. Mol. Plant **15:** 1192–1210.

Takahashi, Y., Zhang, J., Hsu, P.K., Ceciliato, P.H.O., Zhang, L., Dubeaux, G., Munemasa, S., Ge, C., Zhao, Y., Hauser, F., et al. (2020). MAP3Kinase-dependent SnRK2-kinase activation is required for abscisic acid signal transduction and rapid osmotic stress response. Nat. Commun. **11:** 12.

Tardieu, F., Simonneau, T., and Muller, B. (2018). The physiological basis of drought tolerance in crop plants: A scenario-dependent probabilistic approach. Annu. Rev. Plant Biol. **69:** 733–759.

Tester, M., and Langridge, P. (2010). Breeding technologies to increase crop production in a changing world. Science **327:** 818–822.

Tsugama, D., Liu, S., and Takano, T. (2012). A putative myristoylated 2C-type protein phosphatase, PP2C74, interacts with SnRK1 in *Arabidopsis*. FEBS Lett. **586:** 693–698.

Uga, Y., Sugimoto, K., Ogawa, S., Rane, J., Ishitani, M., Hara, N., Kitomi, Y., Inukai, Y., Ono, K., Kanno, N., et al. (2013). Control of root system architecture by *DEEPER ROOTING 1* increases rice yield under drought conditions. Nat. Genet. **45:** 1097–1102.

Vahisalu, T., Kollist, H., Wang, Y.F., Nishimura, N., Chan, W.Y., Valerio, G., Lamminmaki, A., Brosche, M., Moldau, H., Desikan, R., et al. (2008). SLAC1 is required for plant guard cell S-type anion channel function in stomatal signalling. Nature **452:** 487–491.

Wang, H., Tang, J., Liu, J., Hu, J., Liu, J., Chen, Y., Cai, Z., and Wang, X. (2018a). Abscisic acid signaling inhibits brassinosteroid signaling through dampening the dephosphorylation of BIN2 by ABI1 and ABI2. Mol. Plant **11:** 315–325.

Wang, J., Li, C., Li, L., Reynolds, M., Mao, X., and Jing, R. (2021a). Exploitation of drought tolerance-related genes for crop improvement. Int. J. Mol. Sci. **22:** 10265.

Wang, J., Li, L., Li, C., Yang, X., Xue, Y., Zhu, Z., Mao, X., and Jing, R. (2021b). A transposon in the vacuolar sorting receptor gene *TaVSR1-B* promoter region is associated with wheat root depth at booting stage. Plant Biotechnol. J. **19:** 1456–1467.

Wang, J., Li, Q., Mao, X., Li, A., and Jing, R. (2016a). Wheat transcription factor TaAREB3 participates in drought and freezing tolerances in *Arabidopsis*. Int. J. Biol. Sci. **12:** 257–269.

Wang, J., Mao, X., Wang, R., Li, A., Zhao, G., Zhao, J., and Jing, R. (2019a). Identification of wheat stress-responding genes and *TaPR-1-1* function by screening a cDNA yeast library prepared following abiotic stress. Sci. Rep. **9:** 141.

Wang, J., Wang, R., Mao, X., Li, L., Chang, X., Zhang, X., and Jing, R. (2019b). *TaARF4* genes are linked to root growth and plant height in wheat. Ann. Bot. **124:** 903–915.

Wang, K., He, J., Zhao, Y., Wu, T., Zhou, X., Ding, Y., Kong, L., Wang, X., Wang, Y., Li, J., et al. (2018b). EAR1 negatively regulates ABA signaling by enhancing 2C protein phosphatase activity. Plant Cell **30:** 815–834.

Wang, X., Guo, C., Peng, J., Li, C., Wan, F., Zhang, S., Zhou, Y., Yan, Y., Qi, L., Sun, K., et al. (2019c). ABRE-BINDING FACTORS play a role in the feedback regulation of ABA signaling by mediating rapid ABA induction of ABA co-receptor genes. New Phytol. **221:** 341–355.

Wang, X., Wang, H., Liu, S., Ferjani, A., Li, J., Yan, J., Yang, X., and Qin, F. (2016b). Genetic variation in *ZmVPP1* contributes to drought tolerance in maize seedlings. Nat. Genet. **48:** 1233–1241.

Wang, Z., Ren, Z., Cheng, C., Wang, T., Ji, H., Zhao, Y., Deng, Z., Zhi, L., Lu, J., Wu, X., et al. (2020). Counteraction of ABA-mediated inhibition of seed germination and seedling establishment by ABA signaling terminator in *Arabidopsis*. Mol. Plant **13:** 1284–1297.

Wang, Z.P., Xing, H.L., Dong, L., Zhang, H.Y., Han, C.Y., Wang, X. C., and Chen, Q.J. (2015). Egg cell-specific promoter-controlled CRISPR/Cas9 efficiently generates homozygous mutants for multiple target genes in *Arabidopsis* in a single generation. Genome Biol. **16:** 144.

Xiong, L., Ishitani, M., Lee, H., and Zhu, J.K. (2001). The *Arabidopsis* LOS5/ABA3 locus encodes a molybdenum cofactor sulfurase and modulates cold stress- and osmotic stress-responsive gene expression. Plant Cell **13:** 2063–2083.

Yang, J., He, H., He, Y., Zheng, Q., Li, Q., Feng, X., Wang, P., Qin, G., Gu, Y., Wu, P., et al. (2021). TMK1-based auxin signaling regulates abscisic acid responses via phosphorylating ABI1/2 in *Arabidopsis*. Proc. Natl. Acad. Sci. U.S.A. **118:** e2102544118.

Yang, Y., Al-Baidhani, H.H.J., Harris, J., Riboni, M., Li, Y., Mazonka, I., Bazanova, N., Chirkova, L., Sarfraz Hussain, S., Hrmova, M., et al. (2020). *DREB/CBF* expression in wheat and barley using the stress-inducible promoters of *HD-Zip I* genes: Impact on plant development, stress tolerance and yield. Plant Biotechnol. J. **18:** 829–844.

Ye, H., Song, L., Schapaugh, W.T., Ali, M.L., Sinclair, T.R., Riar, M.K., Raymond, R.N., Li, Y., Vuong, T., Valliyodan, B., et al. (2020). The importance of slow canopy wilting in drought tolerance in soybean. J. Exp. Bot. **71:** 642–652.

Yoo, S.D., Cho, Y.H., and Sheen, J. (2007). Arabidopsis mesophyll protoplasts: A versatile cell system for transient gene expression analysis. Nat. Protoc. **2:** 1565–1572.

Yu, F., Qian, L., Nibau, C., Duan, Q., Kita, D., Levasseur, K., Li, X., Lu, C., Li, H., Hou, C., et al. (2012). FERONIA receptor kinase pathway suppresses abscisic acid signaling in *Arabidopsis* by activating ABI2 phosphatase. Proc. Natl. Acad. Sci. U.S.A. **109:** 14693–14698.

Yu, X., Han, J., Li, L., Zhang, Q., Yang, G., and He, G. (2020). Wheat PP2C-a10 regulates seed germination and drought tolerance in transgenic *Arabidopsis*. Plant Cell Rep. **39:** 635–651.

Yu, X., Han, J., Wang, E., Xiao, J., Hu, R., Yang, G., and He, G. (2019). Genome-wide identification and homoeologous expression analysis of PP2C genes in wheat (*Triticum aestivum* L.). Front. Genet. **10:** 561.

Zhang, B., Shi, W., Li, W., Chang, X., and Jing, R. (2013). Efficacy of pyramiding elite alleles for dynamic development of plant height in common wheat. Mol. Breed. **32:** 327–338.

Zhang, H., Ohyama, K., Boudet, J., Chen, Z., Yang, J., Zhang, M., Muranaka, T., Maurel, C., Zhu, J.K., and Gong, Z. (2008a). Dolichol biosynthesis and its effects on the unfolded protein response and abiotic stress resistance in *Arabidopsis*. Plant Cell **20:** 1879–1898.

Zhang, H., Zhu, J., Gong, Z., and Zhu, J.K. (2022). Abiotic stress responses in plants. Nat. Rev. Genet. **23:** 104–119.

Zhang, M., Henquet, M., Chen, Z., Zhang, H., Zhang, Y., Ren, X., van der Krol, S., Gonneau, M., Bosch, D., and Gong, Z. (2009). *LEW3*, encoding a putative alpha-1,2-mannosyltransferase (ALG11) in N-linked glycoprotein, plays vital roles in cell-wall biosynthesis and the abiotic stress response in *Arabidopsis thaliana*. Plant J. **60:** 983–999.

Zhang, Y., Andralojc, P.J., Hey, S.J., Primavesi, L.F., Specht, M., Koehler, J., Parry, M.A.J., and Halford, N.G. (2008b). *Arabidopsis* sucrose non-fermenting-1-related protein kinase-1 and calcium-dependent protein kinase phosphorylate conserved target sites in ABA response element binding proteins. Ann. Appl. Biol. **153:** 401–409.

Zhang, Y., Wang, J., Li, Y., Zhang, Z., Yang, L., Wang, M., Zhang, Y., Zhang, J., Li, C., Li, L., et al. (2023). Wheat TaSnRK2.10 phosphorylates TaERD15 and TaENO1 and confers drought tolerance when overexpressed in rice. Plant Physiol. **191:** 1344–1364.

Zhu, H., Li, C., and Gao, C. (2020). Applications of CRISPR-Cas in agriculture and plant biotechnology. Nat. Rev. Mol. Cell Biol. **21:** 661–677.

SUPPORTING INFORMATION

Additional Supporting Information may be found online in the supporting information tab for this article: http://onlinelibrary.wiley.com/doi/10.1111/jipb.13504/suppinfo

Figure S1. Wilting phenotype of the F_2 population seedlings under drought
Figure S2. Distribution of single-nucleotide polymorphisms (SNPs) on wheat chromosomes
Figure S3. DIW1 belongs to the protein phosphatase 2C family
Figure S4. Expression of *DIW1* in wild-type Fielder, *PP2C-MT* overexpression lines OE2, OE3, and OE5
Figure S5. *TaPP2C158* mutant lines created through CRISPR/Cas9
Figure S6. Expression pattern of *TaPP2C158* in wheat
Figure S7. TaPP2C158 does not interact with TaPYL4 with or without abscisic acid (ABA) in the yeast-two-hybrid assay
Figure S8. Subcellular localization of TaPP2C158 protein
Figure S9. *snrk1.1* mutant line created through CRISPR/Cas9
Figure S10. TaPP2C158 cannot de-phosphorylate TaSnRK2.10 *in vitro*
Figure S11. *Cis* element analysis of the *TaRAB18* promoter
Figure S12. Differences in canopy temperature and seedling survival rate under drought stress based on the SNP at 4221 bp
Table S1. Annotation of candidate genes in the 43.4 kb block on chromosome 5A
Table S2. Detailed information on yeast-two-hybrid screening
Table S3. *TaPP2C158* haplotypes of 323 wheat accessions (Population 1)

Table S4. Association of two polymorphic loci with canopy temperature
Table S5. Association of two polymorphic loci with seedling survival rates (SR)
Table S6. *TaPP2C158* haplotypes of DH lines (Population 2)
Table S7. *TaPP2C158* haplotypes of 157 wheat landraces (Population 3)
Table S8. *TaPP2C158* haplotypes of 348 modern wheat cultivars (Population 4)
Table S9. Primers used in the study

Scan using WeChat with your smartphone to view JIPB online

Scan with iPhone or iPad to view JIPB online